Int. J. Appl. Comput. Math (2025) 11:225
https://doi.org/10.1007/s40819-025-01899-6

ORIGINAL PAPER

A Sex-Structured Mmathematical Model of Mosquito Infection with Microsporidia MB: Model Reduction and Release Strategies

Dhorasso Temfack[1] · Berge Tsanou[2,3] · Jean Lubuma[4] · Mouhamadou Diaby[5]

Accepted: 25 March 2025

Abstract
Malaria remains a significant public health burden in Sub-Saharan African countries, hindering their development. With no effective vaccine currently available, controlling the malaria vector population remains the most effective preventive measure. A promising strategy to combat this disease involves the use of the bacterium *Microsporidia MB* to reduce/replace disease-transmitting wild mosquito population. In this paper, we develop a dynamic model to analyze the transmission dynamics of *Microsporidia MB* within the wild mosquito population, considering both imperfect maternal and horizontal transmissions. In this paper, we develop a dynamic mathematical model to analyze the transmission dynamics of *Microsporidia MB* within wild mosquito populations, accounting for both imperfect maternal and horizontal transmission. We derive and analyze a threshold condition to assess the potential for *Microsporidia MB*-infected mosquitoes to invade and persist in the wild population. By establishing conditions for the local stability of equilibrium points, we explore the influence of maternal transmission on the spread of *Microsporidia MB*. Additionally, we employ a cascade reduction approach to simplify the model into a two-dimensional system and formulate an optimal control problem. Using Pontryagin's Maximum Principle, we determine optimal release strategies for infected mosquitoes to either replace the wild population or promote coexistence with a significantly reduced wild mosquito population. Through theo-

✉ Berge Tsanou
bergetsanou@gmail.com

Dhorasso Temfack
temfackd@tcd.ie

Jean Lubuma
jean.lubuma@wits.ac.za

Mouhamadou Diaby
mouhamadou.diaby@ugb.edu.sn

1 School of Computer Science and Statistics, Trinity College Dublin, Dublin, Ireland

2 Department of Mathematics and Computer Science, University of Dschang, Dschang, Cameroon

3 Department of Mathematics and Applied Mathematics, University of Pretoria, Pretoria, South Africa

4 School of Computer Science and Applied Mathematics , University of the Witwatersrand, Johannesburg, South Africa

5 Department of Applied Mathematics, Gaston Berger University, Saint-Louis, Senegal

Published online: 13 October 2025

retical analysis and numerical simulations, our findings contribute to the understanding and development of effective strategies for malaria control using *Microsporidia MB*.

Keywords *Microsporidia MB* · Maternal transmission · Horizontal transmission · Stability · Optimal control

Introduction

Vector-borne diseases continue to pose significant challenges to global public health, with malaria standing as one of the most formidable examples [1, 2]. Sub-Saharan Africa bears the brunt of this burden, with approximately 95% of malaria cases reported in the region [3]. Transmitted through the bites of infected Anopheles mosquitoes, malaria causes extensive morbidity and mortality, particularly among young children and pregnant women [3]. Although conventional interventions, such as insecticide-based approaches, have been instrumental in malaria control, the emergence of insecticide resistance and environmental concerns necessitate the exploration of alternative strategies. One promising avenue involves harnessing the power of symbiotic microorganisms to disrupt malaria transmission. In recent years, the symbiotic bacterium *Microsporidia MB* has emerged as a potential tool for malaria control [4, 5]. This maternally inherited bacterium infects mosquitoes and imparts resistance against the malaria parasite, thereby reducing their capacity to transmit the disease. The concept entails releasing *Microsporidia MB*-infected mosquitoes into the wild, with the goal of either replacing or significantly reducing the population of disease-transmitting mosquitoes. Mathematical modeling plays a pivotal role in comprehending the intricate dynamics of infectious diseases and evaluating the efficacy of control strategies. The idea of utilizing symbiotic microorganisms for vector-borne disease control has been successfully demonstrated in other contexts. For instance, field trials in Guangzhou have shown that the *Wolbachia* symbiont effectively reduces the ability of *Aedes aegypti* mosquitoes to transmit dengue fever [6, 7]. This success has spurred extensive research into the theoretical dynamics of *Wolbachia* spread and its potential for mosquito population replacement and disease suppression [8–10]. Various mathematical models, including difference and differential equation-based frameworks, have been developed to evaluate mosquito release strategies for *Wolbachia*-based control [11, 12]. These models incorporate key biological mechanisms such as cytoplasmic incompatibility (which prevents hatching of eggs from uninfected females mated with infected males), incomplete maternal transmission, and infection reversion dynamics [13, 14]. Some studies have also investigated the potential of using *Wolbachia* to control the spread of malaria [15]. The study by Florez et al. [16] suggests that the most efficient approach to establishing *Wolbachia* within *Anopheles albimanus* mosquito populations in Haiti is to release all infected mosquitoes immediately after the prerelease mitigation process. Given the biological and functional similarities between *Microsporidia MB* and *Wolbachia*, it is important to investigate whether the mathematical models developed for *Wolbachia*-based control of dengue can be adapted to study *Microsporidia MB*-mediated malaria vector control. Additionally, understanding how the unique transmission mechanisms of *Microsporidia MB* influence its spread is crucial, as they may lead to higher prevalence, population replacement, or significant suppression of wild mosquito populations. While previous studies have explored the impact of *Wolbachia* on mosquito population dynamics and disease transmission, the dynamics of *Microsporidia MB* remain largely unexplored. In this paper, we address this gap by introducing a novel mathematical model that captures the unique transmission dynamics

of *Microsporidia MB* and its interaction with wild mosquito populations. Our contributions are threefold: (i) We develop a comprehensive mathematical framework to characterize the spread of *Microsporidia MB* within mosquito populations, incorporating its distinct modes of transmission. (ii) We derive and analyze key epidemiological thresholds, including the basic reproduction number ($\mathcal{R}_0$), to assess conditions under which *Microsporidia MB* can establish itself and lead to population replacement or suppression. (iii) We propose a model reduction scheme and investigate different mosquito release strategies, identifying optimal control measures that maximize the effectiveness of *Microsporidia MB* in reducing malaria vector populations.

The subsequent sections of this paper are organized as follows: "Model Formulation" section, we present a comprehensive mathematical analysis of our proposed model, encompassing both theoretical and epidemiological aspects. In "Cascade of Reduced Models" section, we present step-by-step reduction techniques to simplify the original model. "Analysis of the Complete Model and Comparison with Reduced Models", we perform a comprehensive mathematical analysis of the proposed model and compare the simplified models with the original one. Finally, in "Mosquito Release Strategies" section, we explore diverse strategies for controlling the population of wild mosquitoes, considering both theoretical implications and practical applications. By investigating the transmission dynamics of *Microsporidia MB* and evaluating control strategies, this study aims to contribute to the development of effective interventions for malaria vector control.

Ecological Background on Microsporidia MB

In the ongoing effort to combat vector-borne diseases, an exciting breakthrough has been made by a team of researchers from the United Kingdom and Kenya. During their study, they serendipitously discovered a microbe known as *Microsporidia MB* on the shores of Lake Victoria. This microbe possesses a remarkable ability to immunize Anopheles mosquitoes against malaria [17]. Notably, it selectively targets the Anopheles gambiae and arabiensis species, which are the primary carriers of malaria. Interestingly, *Microsporidia MB* naturally coexists with a symbiotic bacterium/fungi found in approximately 5% of Anopheles mosquito species. Experimental findings have revealed that infections caused by *Microsporidia MB* persist throughout the mosquito's entire lifespan and become more potent as the mosquito ages, resulting in long-term protection against malaria [18]. Unlike the *Wolbachia* bacterium, which can impact mosquito fecundity and lifespan, *Microsporidia MB* infections do not lead to any reduction in reproductive capacity or lifespan, nor do they induce cytoplasmic incompatibility [17].

Furthermore, it has been observed that horizontally infected females can transmit *Microsporidia MB* to their offspring at a relatively high rate [18]. This unique characteristic, coupled with the microbe's double mode of transmission, positions *Microsporidia MB* as a promising contender for the biological control of malaria transmission. More specifically, the *Microsporidia MB* is an infecting microbe of mosquitoes having the following characteristics [17]:

- It is a symbiotic bacterium/fungi naturally present in about 5% Anopheles mosquito species.
- It blocks the transmission of Plasmoduim from mosquitoes to humans.
- It is transmitted vertically from mother to offspring.

- It is (sexually) transmitted horizontally and bi-directionally during mating between adult mosquitoes.
- It incurs no fitness cost on its host: it does affect significantly the lifespan and fertility of infected mosquitoes.
- Its infection does not induce virulence to the infected mosquitoes.

These features should be carefully accounted for when modeling its dynamics within the wild mosquito population.

Model Formulation

Our mathematical model extends existing frameworks developed for *Wolbachia* transmission [4, 19, 20], while incorporating the distinctive characteristics of *Microsporidia MB* transmission. Unlike *Wolbachia*, which predominantly relies on maternal transmission, *Microsporidia MB* exhibits horizontal transmission among mosquitoes [18], and it does not induce the cytoplasmic incompatibility phenomenon [21]. The core strategy of our model involves the introduction of *Microsporidia MB*-infected wild mosquitoes into the population. Specifically, we extend and enrich the seminal model in [11] given below (for the convenience of the reader, see Fig. 1 and system (1)), by splitting the mosquito population into two groups.

$$\begin{cases} \frac{dA}{dt} = \phi F\left(1 - \frac{A}{K_a}\right) - (\gamma + \mu_a)A, \\ \frac{dF}{dt} = b_f \gamma A - \mu_f F, \\ \frac{dM}{dt} = b_m \gamma A - \mu_m M. \end{cases} \tag{1}$$

In order to build the sex-structured model for *microsporidia MB* infection, we split the mosquito population into two groups. One group for the uninfected mosquitoes and the other for *microsporidia MB*-infected mosquitoes. For the uninfected group, we follow the baseline model (1) above, and define the population of uninfected wild mosquitoes in the aquatic stage, adult females, and adult males as A_u, F_u, and M_u. Correspondingly, for the infected group, we denote the population of *Microsporidia MB*-infected mosquitoes in the aquatic stage, adult females, and adult males as A_i, F_i, and M_i. Additionally, we enrich the baseline model (1) by explicitly modeling the different mating processes between females and males of within and across the mosquito groups. We further assume a spatially homogeneous distribution of mosquitoes throughout the population. Upon a female mosquito mating with a random male mosquito, the probability of the male being uninfected is given by $M_u/(M_u + M_i)$, whereas the probability of the male being infected is given by $M_i/(M_u + M_i)$. As mentioned earlier, unlike some symbiotic bacteria like *Wolbachia*, *Microsporidia MB* infection does not induce the cytoplasmic incompatibility phenomenon [21]. Therefore, the mating between an uninfected female mosquito and an infected male may result in oviposition by the female and production of offspring. However, experimental data indicate that maternal transmission of *Microsporidia MB*, as a result of all these mating processes, is imperfect [18]. This is accounted for here by introducing parameters ρ_1, ρ_2, and ρ_3. In fact, we assume that mating between infected males (M_i) and infected females (F_i) consistently produces a fraction ρ_1 of infected offspring. Correspondingly, we assume that mating between uninfected males (M_u) and infected females (F_i) always results in a fraction ρ_2 of infected offspring. Finally, we assume that mating between infected males (M_i) and uninfected females (F_u) may or may not lead to female infection, depending on the probability λ_m, followed by a fraction ρ_3 of infected offspring as shown in Fig. 2. When $\lambda_m = 0$, no transmission occurs, and the

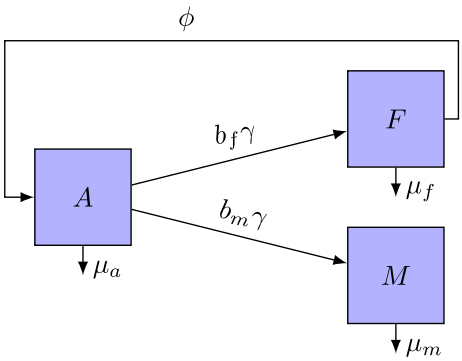

Fig. 1 The baseline model for mosquito dynamics. *The variable A represents the mosquito population at the aquatic stage*; *F and M are respectively the emerging female and male mosquito populations. When breeding sites are abundant, female mosquito spawning rate is defined by* ϕ. *This ovoposition rate is limited by an environmental carrying capacity* K_a *which depends on the availability of egg laying sites and environmental resources. Mosquitoes grow from the aquatic stage to the adult stage at a rate* γ *and a fraction* b_f *are females while the remaining fraction* $b_m = 1 - b_f$ *are males. The parameters* μ_a, μ_f *and* μ_m *denote the per capacity mortality of mosquitoes at the aquatic stage, female adult mosquitoes and adult male mosquitoes, respectively*

resulting offspring are completely uninfected. Of course, mating between uninfected males (M_u) and uninfected females (F_u) always produces entirely uninfected offspring. Our main model assumptions include the fertility of all female mosquitoes, the persistent *Microsporidia MB* infection throughout the mosquito lifespan; disregard the mosquito migration, neglect the incubation period for horizontally acquired *Microsporidia MB* infection, account for the equal development rate in the aquatic stage for infected and uninfected mosquitoes, and assume a mating frequency of one for both uninfected/infected females and uninfected/infected males. Notably, *Microsporidia MB* infection does not impose a fitness cost on mosquitoes [17], maintaining consistent birth and death parameters for both (infected and uninfected) mosquito populations.

We summarize in Table 1 the different offspring proportions of mosquito ticks according to the four possible types of matings.

The parameters ρ_1, ρ_2 and ρ_3 ($\rho_3 < \rho_2 \leq \rho_1$) translating the efficiency of the maternal transmission are all included in the interval (0, 1]. The cases $\rho_i = 1, i \in \{1, 2, 3\}$ correspond to a perfect maternal transmission.

Under the above assumptions, the sex-structured model of the transmission of *Microsporidia MB* within the mosquito population is given by the following system of differential equations:

Table 1 Mating strategies and their offspring probabilities

Male	Female	Fraction of infected offspring	Fraction of uninfected offspring
Uninfected	Uninfected	0	1
Infected	Uninfected	$\rho_3\lambda_m$	$1-\rho_3\lambda_m$
Uninfected	**Infected**	ρ_2	$1-\rho_2$
Infected	**Infected**	ρ_1	$1-\rho_1$

The bold indicate MB-infected mosquitoes

$$\begin{cases} \dfrac{dA_u}{dt} = \phi\left(\dfrac{M_uF_u + (1-\rho_1)M_iF_i + (1-\rho_2)M_uF_i + (1-\rho_3\lambda_m)M_iF_u}{M_u+M_i}\right)\left(1-\dfrac{A}{K_a}\right) \\ -(\gamma+\mu_a)A_u, \\ \dfrac{dA_i}{dt} = \phi\left(\dfrac{\rho_1M_iF_i + \rho_2M_uF_i + \rho_3\lambda_mM_iF_u}{M_u+M_i}\right)\left(1-\dfrac{A}{K_a}\right) - (\gamma+\mu_a)A_i, \\ \dfrac{dF_u}{dt} = b_f\gamma A_u - \beta_m\dfrac{M_i}{M_u+M_i}F_u - \mu_fF_u, \\ \dfrac{dF_i}{dt} = b_f\gamma A_i + \beta_m\dfrac{M_i}{M_u+M_i}F_u - \mu_fF_i, \\ \dfrac{dM_u}{dt} = b_m\gamma A_u - \beta_f\dfrac{F_i}{F_u+F_i}M_u - \mu_mM_u, \\ \dfrac{dM_i}{dt} = b_m\gamma A_i + \beta_f\dfrac{F_i}{F_u+F_i}M_u - \mu_mM_i. \end{cases} \tag{2}$$

In System (2), $A = A_u + A_i$ is the total number of mosquitoes in aquatic stage which is assumed to be always smaller than the environmental carrying capacity K_a. We give in Table 2 the description of all the parameters in the system (2). The first block in the right hand side of the second equation of (2), models the vertical transmission of the infection according to the different matings performed, in which, for instance, the term

$$\phi\rho_3\lambda_m\frac{M_iF_u}{M_u+M_i}\left(1-\frac{A}{K_a}\right),$$

represents the number of mosquitoes in aquatic stage produced by an uninfected female having acquired the infection horizontally. The latter quantity is only visible in the specific case of *Microsporidia MB*, due to the possibility of vertical transmission after horizontal acquisition of infection. The remaining terms in that first block are defined similarly and the same reasoning applies for the first block of the right hand side of the first equation. The terms

$$\beta_m\frac{M_i}{M_u+M_i}F_u \text{ and } \beta_f\frac{F_i}{F_u+F_i}M_u$$

in the last four equations of the system (2), model the horizontal bidirectional transmission of *Microsporidia MB* infection during mating. This is a clear extension of the baseline model (1) by accounting for the horizontal transmission of *Microsporidia MB*.

We shall show that the set $\mathcal{D}$ below is the biological meaningful domain in the precise sense of Theorem 1, Proposition 1 and Corrollary 1 in "Analysis of the Complete Model and

Table 2 Descrtiption of the parameters of the model (2)

Param.	Biological description	Baseline	Range	Reference
K_a	Aquatic stage carrying capacity	2×10^5	$[10^3-10^6]$	Assumed*
ϕ	Per capita laying rate of eggs for F_u and F_i	20	[10−55]	[20, 22]
ρ_1	Fraction of egg infected from mating $M_i \times F_i$	0.76	[0.5−1]	Assumed*
ρ_2	Fraction of infected egg from mating $M_u \times F_i$	0.45	[0.4−1]	Assumed*
ρ_3	Fraction of infected egg from mating $M_i \times F_u$	0.37	[0.3−1]	[18]
λ_m	Probability that contact between M_i and F_u is infectious	0.516	[0.36−1]	[18]
β_m	Horizontal infection rate of infected males to females	0.04	[0.02−0.05]	Assumed*
β_f	Horizontal infection rate from infected females to males	0.026	[0.01−0.05]	Assumed*
b_f	Fraction of eggs that are female	0.5	[0.5−0.58]	[20, 22]
b_m	Fraction of eggs that are male $(= 1 - b_f)$	0.5	[0.042−0.5]	[20, 22]
γ	Maturation rate of the mosquito to the aquatic stage	0.11	[0.07−0.25]	[20, 22]
μ_a	Per capita aquatic mortality rate	0.025	–	[20, 22]
μ_f	Per capita death rate of female mosquitoes	0.1	[0.07−0.14]	[20, 22]
μ_m	Per capita death rate of male mosquitoes	0.14	[0.06−0.14]	[20, 22]

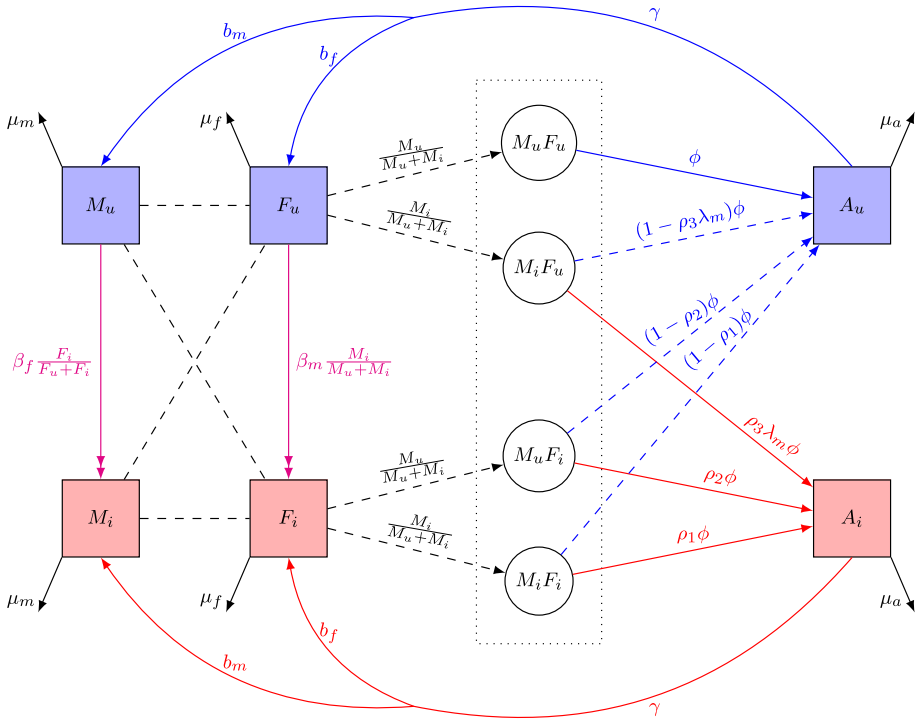

Fig. 2 Transmission dynamics of *Microsporidia MB* . *Uninfected mosquitoes at the aquatic stage, females, and males are represented by blue compartments* (A_u, F_u, M_u)*, while infected mosquitoes at the aquatic stage, females, and males are represented by red compartments* (A_i, F_i, M_i)*. Mating events between infected and uninfected mosquitoes, leading to infection of the uninfected partner, are denoted by black circles with infection rates* β_m *or* β_f*. The blue and red lines show the population dynamics of uninfected and infected mosquitoes, respectively. Purple lines represent horizontal transmission, originating from the* M_u *and* F_i *compartments. Imperfect maternal transmission is indicated by blue dotted lines. Mortality rates for mosquitoes are shown by black lines exiting the compartments. Female mosquitoes lay eggs at a rate* ϕ*, and mosquitoes develop from the aquatic stage to the adult stage at a rate* γ*, with a fraction* b_f *becoming females and the remaining fraction* $b_m = 1 - b_f$ *becoming males*

Comparison with Reduced Models" section.

$$\mathcal{D} = \left\{ \begin{pmatrix} A_u \\ A_i \\ F_u \\ F_i \\ M_u \\ M_i \end{pmatrix} \in \mathbb{R}^6 \middle| \begin{array}{l} A_u > 0, \\ A_i \geq 0, \\ 0 \leq A_u + A_i \leq K_a, \\ F_u > 0, \\ F_i \geq 0, \\ 0 < F_u + F_i \leq \dfrac{b_f \gamma K_a}{\mu_f}, \\ M_u > 0, \\ M_i \geq 0, \\ 0 < M_u + M_i \leq \dfrac{b_m \gamma K_a}{\mu_m} \end{array} \right\} \tag{3}$$

Before going further and deeper in the analysis of System (2), we need the following two ecological thresholds. We denote by $\mathcal{R}_u$ and $\mathcal{R}_i$ the next generation number (basic offspring

number) for the uninfected and infected of mosquito population, respectively. They are given by the following expressions:

$$\mathcal{R}_u = b_f \frac{\gamma}{(\gamma + \mu_a)} \frac{\phi}{\mu_f}, \quad \text{and} \quad \mathcal{R}_i = \rho_1 b_f \frac{\gamma}{(\gamma + \mu_a)} \frac{\phi}{\mu_f}. \tag{4}$$

More specifically, the quantity $\mathcal{R}_u$ measures the number of uninfected eggs produced by an uninfected female during her life cycle and determines ability of wild mosquitoes persist or disappear, while $\mathcal{R}_i$ measures the number of infected eggs produced by an infected female during her life cycle and determines the ability of *Microsporidia MB* infected mosquitoes to persist or die out.

Given the intrinsic complexity of the mathematical system (2), it is both useful and relevant to simplify the it by using some biological properties of the mosquito life cycle. Moreover, it is difficult to perform the theoretical analysis that system of six highly non-linear differential equations. This motivates us to create in the next section, a cascade of reduced models based on assumptions that hold for a range of parameters and initial conditions appropriate for real-world applications.

Cascade of Reduced Models

In this section, we aim to simplify the original model by reducing it to a more concise form while preserving its key parameters. We mimic a reduction techniques in [23], which involves eliminating the aquatic stage of the mosquito and reducing the number of variables.

Suppression of the Aquatic Stage: Reduction to 4-Dimensional System

Since the transmission of *Microsporidia MB* occurs primarily between adult mosquitoes or vertically from infected females to their offspring, the population of mosquitoes in the aquatic stage does not directly contribute to the transmission dynamics of the infection. Therefore, we can simplify the model by removing the aquatic compartments (A_u and A_i) and assuming instantaneous hatching of eggs into adult mosquitoes [23]. However, in contrast to the approach taken in [23], we consider that the total lifespan of a mosquito does not include the time spent in the aquatic stage. Hence, in the reduced model, we retain the mortality rates of male and female mosquitoes as μ_m and μ_f respectively.

To determine the basic reproduction numbers of the uninfected and infected mosquito populations in the absence of interaction between the two populations in the reduced model without the aquatic stage, we define $\mathcal{R}_u^{(4)}$ and $\mathcal{R}_i^{(4)}$ as:

$$\mathcal{R}_u^{(4)} = b_f \frac{\phi_u'}{\mu_f}, \quad \text{and} \quad \mathcal{R}_i^{(4)} = \rho_1 b_f \frac{\phi_i'}{\mu_f}. \tag{5}$$

Here, $\mathcal{R}_u^{(4)}$ represents the number of uninfected offspring produced by an uninfected female during her lifetime, while $\mathcal{R}_i^{(4)}$ represents the number of infected offspring produced by an infected female during her lifetime. The parameters ϕ_u' and ϕ_i' denote the average rates of offspring produced by an uninfected and infected female, respectively. To preserve the key parameters of the model, we impose that the reproductive rates of the population in the reduced model are the same as those in the initial model (2), leading to the relationship:

$$\phi' = \phi_u' = \phi_i' = \frac{\gamma}{\gamma + \mu_a} \phi. \tag{6}$$

Here, ϕ' represents the average rate of offspring produced by a female during her life cycle. Considering that the growth of the mosquito population is influenced by the ability of females (both uninfected and infected) to find suitable egg-laying sites, which can accommodate only a limited number of females, we substitute the environmental carrying capacity K_a of mosquitoes in the aquatic stage with the environmental carrying capacity K of female mosquitoes:

$$K = b_f \frac{\gamma}{\mu_f} K_a. \tag{7}$$

The value of K corresponds to the maximum number of females (uninfected and infected) that the environment can sustain. By skillfully eliminating the equations for the aquatic stage (A_u, A_i) and utilizing certain biological characteristics of the mosquito life cycle, we can capture the dynamics of the aquatic stage at the adult stage.

To achieve this, we make the following assumptions and approximations:

- Firstly, we replace the mosquito renewal rate in the aquatic stage with the female renewal rate at the adult stage, which is a more biologically meaningful quantity since females are responsible for oviposition. To accomplish this, we approximate the logistic term $\left(1 - \frac{A_u+A_i}{K_a}\right)$ by $\left(1 - \frac{F_u+F_i}{K}\right)$ in two first equation of (2).
- Secondly, we assume that the oviposition rate ϕ of females and the egg hatching rate γ are much greater than their respective mortality rates. As a result, we assume that the aquatic compartments A_u and A_i are fast variables and their dynamics of eggs are at equilibrium. They are then approximated by the following expressions:

$$\begin{aligned}
A_u &\sim \frac{\phi}{\gamma+\mu_a}\left(\frac{M_u F_u + (1-\rho_1)M_i F_i + (1-\rho_2)M_u F_i + (1-\rho_3\lambda_m)M_i F_u}{M_u + M_i}\right)\left(1 - \frac{F_u+F_i}{K}\right)\\
A_i &\sim \frac{\phi}{\gamma+\mu_a}\left(\frac{\rho_1 M_i F_i + \rho_2 M_u F_i + \rho_3\lambda_m M_i F_u}{M_u + M_i}\right)\left(1 - \frac{F_u+F_i}{K}\right).
\end{aligned}$$

These approximations allow us to effectively capture the dynamics of the aquatic stage at the adult stage, while simplifying the model by removing explicit equations for A_u and A_i. By incorporating these assumptions and approximations, we can analyze the simplified model (2) more conveniently, as we focus on the adult stage dynamics and capture the essential aspects of the mosquito life cycle.

The reduced model without the aquatic stage for the transmission of the *Microsporidia MB* infection is therefore given by the following 4-**ODE** system:

$$\begin{cases}
\frac{dF_u}{dt} = b_f\phi'\left(\frac{M_u F_u + (1-\rho_1)M_i F_i + (1-\rho_2)M_u F_i + (1-\rho_3\lambda_m)M_i F_u}{M_u + M_i}\right)\left(1 - \frac{F}{K}\right)\\
-\beta_m \frac{M_i}{M_u+M_i} F_u - \mu_f F_u,\\
\frac{dF_i}{dt} = b_f\phi'\left(\frac{\rho_1 M_i F_i + \rho_2 M_u F_i + \rho_3\lambda_m M_i F_u}{M_u + M_i}\right)\left(1 - \frac{F}{K}\right) + \beta_m \frac{M_i}{M_u+M_i} F_u - \mu_f F_i,\\
\frac{dM_u}{dt} = b_m\phi'\left(\frac{M_u F_u + (1-\rho_1)M_i F_i + (1-\rho_2)M_u F_i + (1-\rho_3\lambda_m)M_i F_u}{M_u + M_i}\right)\left(1 - \frac{F}{K}\right)\\
-\beta_f \frac{F_i}{F_u+F_i} M_u - \mu_m M_u,\\
\frac{dM_i}{dt} = b_m\phi'\left(\frac{\rho_1 M_i F_i + \rho_2 M_u F_i + \rho_3\lambda_m M_i F_u}{M_u + M_i}\right)\left(1 - \frac{F}{K}\right) + \beta_f \frac{F_i}{F_u+F_i} M_u - \mu_m M_i.
\end{cases} \tag{8}$$

Where $F = F_u + F_i$ represents the total size of the female mosquito population.

Removing Males: Reduction to 2-Dimensional System

Here we wish to reduce the number of variables in the 4-**ODE** model obtained earlier by approximating the fraction of infected males in the total male population as a function of the fraction of infected females in the total female population. Thus the system (8) can be identified as a 2-**ODE** system reflecting the progression of female mosquitoes [23]. To reduce the differential system (8), we first assume that the horizontal infection rate β_m from infected male mosquitoes to females and the horizontal infection rate β_f from infected female mosquitoes to male are equal and we set:

$$\beta_m = \beta_f = \beta, \qquad \text{with} \qquad \beta = \lambda c. \tag{9}$$

Where $\lambda = \lambda_m$ denotes the probability of infection during mating between an infected and an uninfected mosquito and c the contact rate between an infected mosquito and an uninfected mosquito per unit of time.

It is also assumed that male and female mosquitoes have the same birth rate. This is reasonable considering experimental work in [17] which estimates the ratio of male to female mosquitoes to be $1.08 : 1$. So we have $b_f = b_m = \frac{1}{2}$. Since the infection with *Microsporidia MB* is not accompanied by a reduction in the longevity of the mosquito, the above assumptions allow us to consider therefore at the following approximation:

$$\frac{F_i}{F_u + F_i} \approx \frac{M_i}{M_u + M_i} \tag{10}$$

We justify this approximation using numerical simulations (see Fig. 3).

Thus, the reduced model of transmission of *Microsporidia MB* within the female mosquito population is thus written:

$$\begin{cases} \dfrac{dF_u}{dt} = b\left(\dfrac{F_u^2 + (1-\rho_1)F_i^2 + (1-\rho_2)F_uF_i + (1-\rho_3\lambda)F_iF_u}{F_u + F_i}\right)\left(1 - \dfrac{F_u + F_i}{K}\right) \\ -\beta\dfrac{F_i}{F_u + F_i}F_u - \mu_f F_u, \\ \dfrac{dF_i}{dt} = b\left(\dfrac{\rho_1 F_i^2 + \rho_2 F_uF_i + \rho_3\lambda F_iF_u}{F_u + F_i}\right)\left(1 - \dfrac{F_u + F_i}{K}\right) + \beta\dfrac{F_i}{F_u + F_i}F_u - \mu_f F_i. \end{cases} \tag{11}$$

Where $b = b_f\phi'$ denotes the birth rate of female mosquitoes. In the absence of horizontal transmission, model (11) is similar to the model introduced in [24] for the dynamic of *Wolbachia* spread with imperfect maternal transmission and without cytoplasmic incompatibility phenomena.

Analysis of the Complete Model and Comparison with Reduced Models

Assuming female mosquitoes live longer than males and mate only once in their lifetime, we have the following assumptions:

$$\beta_f \leq \beta_m \quad \text{and} \quad \mu_f \leq \mu_m. \tag{12}$$

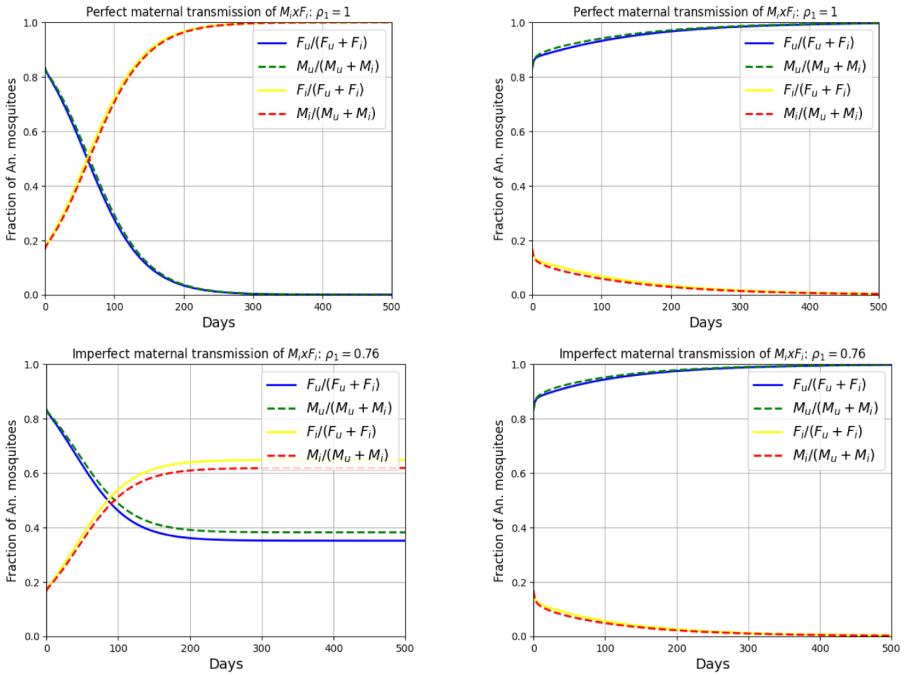

Fig. 3 Proportion of mosquitoes *For the simulation, we choose an transmission of initial infection rate of* 20%. *The figures in the left show the case where we have the dominance of the MB-infected mosquitoes with* $\rho_2 = 0.7$, $\rho_3 = 0.55$, $\lambda = 0.7$. *The figures in the right show the case where we have the extinction of the MB-infected mosquitoes with* $\rho_2 = 0.45$, $\rho_3 = 0.3$, $\lambda = 0.37$. *The other values of the parameters influencing the infection are* $\mu_f = 0.06$, $\mu_m = 0.14$, $\beta = 0.032$. *The small difference between the proportions of males and females being due to differences in mortality rates*

Table 3 Description of the parameters of the model (11) *Here we give the definitions of the parameters newly introduced in the reduced model. The description of the other parameters is given in Table* 2 "*Model Formulation*" *of section*

Parameter	Biological description	Unit
$b = b_f \left(\frac{\gamma}{\gamma+\mu_a}\right)\phi$	Birth rate of female mosquitoes	Mosquito per day
λ	Probability of horizontal infection during mating	Dimensionless
β	Horizontal infection rate	Per day
$K = b_f \frac{\gamma}{\mu_f} K_a$	Carrying capacity of female mosquitoes	Mosquito

Theoretical and Numerical Study of the 6-ODE Model

The system (2) can be expressed as:

$$X' = \mathcal{F}_2(X), \tag{13}$$

with $X = (A_u, A_i, F_u, F_i, M_u, M_i)^T$, The function $\mathcal{F}_2 : \mathbb{R}^6 \longrightarrow \mathbb{R}^6$ represents the right-hand side of (2). We extend the system's domain to include the point $E_0 = 0_{\mathbb{R}^6}$ by defining

$\mathcal{F}_2(E_0) = 0_{\mathbb{R}^6}$, ensuring continuity and existence of a solution for any Cauchy problem associated with (2).

We associate to the system (13) the initial condition: $X(0) = X_0 = (A_u^0, A_i^0, F_u^0, F_i^0, M_u^0, M_i^0)^T$ such that:

$$A_u^0 > 0, \quad A_i^0 \geq 0, \quad F_u^0 > 0, \quad F_i^0 \geq 0, \quad M_u^0 > 0, \quad M_i^0 \geq 0. \tag{14}$$

Global Existence, Positivity and Uniqueness of the Solution

Theorem 1 *For any initial condition in $\mathcal{D}$ and verifying (14), the system (13) has a unique solution that remains in $\mathcal{D}$ for any time $t \geq 0$.*

Proof The function $\mathcal{F}_2$ is of class $\mathcal{C}^1$ in the neighborhood of X_0 and the Cauchy- Lipschitz theorem ensures the existence of a unique solution of the Cauchy problem associated with the system (13) of initial condition X_0.

It remains to show that $\mathcal{D}$ is positively invariant by the flow of the system (13) for any time $t \geq 0$. To do this, we show that the vector field defined by $\mathcal{F}_2$ is either tangential or directed to the interior of $\mathcal{D}$.
Indeed, if

$$\begin{aligned}
&A_u + A_i = K_a \Longrightarrow A_u' + A_i' = -(\gamma + \mu_a)K_a \leq 0,\\
&F_u + F_i = \frac{b_f \gamma K_a}{\mu_f} \Longrightarrow F_u' + F_i' = b_f\gamma(A_u + A_i) - \mu_f(F_u + F_i)\\
&\qquad\qquad \leq b_f\gamma K_a - \mu_f(F_u + F_i) = 0,\\
&M_u + M_i = \frac{b_m \gamma K_a}{\mu_m} \Longrightarrow M_u' + M_i' = b_m\gamma(A_u + A_i) - \mu_m(M_u + M_i)\\
&\qquad\qquad \leq b_m\gamma K_a - \mu_m(M_u + M_i) = 0.
\end{aligned}$$

Futhermore,

$$\begin{aligned}
&A_u = 0 \Longrightarrow A_u' \geq 0 \quad because \quad A = A_u + A_i \leq K_a,\\
&A_i = 0 \Longrightarrow A_i' \geq 0 \quad because \quad A = A_u + A_i \leq K_a,\\
&F_u = 0 \Longrightarrow F_u' \geq 0,\\
&F_i = 0 \Longrightarrow F_i' \geq 0,\\
&M_u = 0 \Longrightarrow M_u' \geq 0,\\
&M_i = 0 \Longrightarrow M_i' \geq 0.
\end{aligned}$$

This proves that on different edges of the domain $\mathcal{D}$, the vector field $\mathcal{F}_2$ points inwards. Thus for any initial condition (14) in $\mathcal{D}$ the solution of (13) remains in $\mathcal{D}$. □

Proposition 1 *The set $\mathcal{D}$ is a basin of attraction relative to the system (13): In other words, $\mathcal{D}$ is an absorbing domain.*

Proof Consider an initial condition of type (14) which does not belong to $\mathcal{D}$. Let $X = (A_u, A_i, F_u, F_i, M_u, M_i)^T$ be the solution of (13) associated to this initial condition.

Since the domain $\mathcal{D}$ is invariant, it is therefore sufficient to show that there exists a time $\tau > 0$ such that $X(\tau) \in \mathcal{D}$.
We pose:

$$A = A_u + A_i, \quad F = F_u + F_i, \quad M = M_u + M_i.$$

– Suppose that for all $t \geq 0$, $A(t) > K_a$. Then we have

$$A'(t) = \phi F(t)\left(1 - \frac{A(t)}{K_a}\right) - (\gamma + \mu_a)A(t)$$
$$\Rightarrow A'(t) \leq -(\gamma + \mu_a)A(t).$$

By applying Gronwall's lemma, we have for all $t \geq 0$

$$A'(t) \leq A(0)e^{-(\gamma+\mu_a)t}.$$

In particular for $t = t_1 = \dfrac{1}{\gamma + \mu_a} \ln\left(\dfrac{A(0)}{K_a}\right) > 0$, we have $A(t_1) \leq K_a$ which is absurd. Hence there exists a first time $t_1' > 0$ such that $\forall t \geq t_1', \quad A(t) \leq K_a$.

– If $F(t_1') \leq \dfrac{b_f \gamma K_a}{\mu_f}$, thus $F(t) \leq \dfrac{b_f \gamma K_a}{\mu_f} \quad \forall t \geq t_1'$ because $\mathcal{D}$ is invariant. Otherwise, suppose that for all $t \geq t_1'$, we have $F(t) > \dfrac{b_f \gamma K_a}{\mu_f}$. Thus

$$F'(t) = b_f \gamma A(t) - \mu_f F(t), \quad \forall t \geq t_1'$$
$$\Rightarrow F'(t) < b_f \gamma (A(t) - Ka) \quad \forall t \geq t_1'.$$

Integrating this inequality over the interval $[t_1', s]$, with $s > t_1'$ fixed, we obtain

$$F(s) \leq F(t_1') - b_f \gamma \int_{t_1'}^{s} (A(t) - K_a)dt.$$

This gives us by applying the integral mean theorem the existence of $s_0 \in [t_1', s]$ such that

$$F(s) \leq F(t_1') + b_f \gamma (A(s_0) - K_a)(s - t_1').$$

In particular for $s = t_2 = t_1 + \dfrac{F(t_1') - \dfrac{b_f \gamma K_a}{\mu_f}}{b_f \gamma (Ka - A(s_0))}$, we have $F(t_2) \leq \dfrac{b_f \gamma K_a}{\mu_f}$ which is absurd and thus there exists a time t_2' such that $\forall\, t \geq t_2'$, $F(t) \leq \dfrac{b_f \gamma K_a}{\mu_f}$.

– In the same way, we show that there exists an instant $t_3' > 0$ such that $\forall t \geq t_3'$, we have $M(t_3') \leq \dfrac{b_m \gamma K_a}{\mu_m}$.

Thus by taking $\tau = \max\{t_1', t_2', t_3'\}$, the solution $X(t)$ remain in $\mathcal{D}$ $\forall t \geq \tau$. □

Corollary 1 *The maximal solution of the Cauchy problem associated with the system (13) of initial condition (14) is global.*

Proof According to the previous proposition and Theorem 1, the unique maximal solution of the Cauchy problem associated to the system (13) of initial condition (14) is bounded. It therefore exists globally for positive times. □

Equilibrium Points

The transmission model of *Microsporidia MB* given by the system (2) has three equilibrium points: the equilibrium point $E_0 = (0, 0, 0, 0, 0, 0)^T$ which corresponds to

extinction of both populations called mosquito free equilibrium (MFE); the equilibrium point $E_u = (A_u^*, 0, F_u^*, 0, M_u^*, 0)^T$ where only wild mosquito population exists and called infection free equilibrium (IFE); according to the level of maternal transmission between infected mosquitoes (perfect or imperfect), we have either the equilibrium point $E_i = (0, A_i^*, 0, F_i^*, 0, M_i^*)^T$ corresponding to a total invasion of the wild mosquito population by mosquitoes infected with *Microsporidia MB* called complete infection equilibrium (CIE), or the point of coexistence of the two mosquito populations $E^c = (A_u^c, A_i^c, F_u^c, F_i^c, M_u^c, M_i^c)^T$ called coexistence equilibrium (CE).

A_1) ***Extinction of both mosquito populations*** The trivial equilibrium point or mosquito-free equilibrium E_0 is not biologically realistic. However, in the absence of interaction between the two mosquito populations (the evolution of each mosquito population does not depend on the other), the growth of each population follows a growth model similar to that studied in [11] and regulated by a reproduction threshold $\mathcal{R}_u$ and $\mathcal{R}_i$.

A_2) ***Wild mosquito population only*** The infection free equilibrium (IFE) is obtained by taking $A_i = F_i = M_i = 0$. It reflects the situation where the mosquitoes carrying the *Microsporidia MB* infection eventually disappear after some time following their introduction into the wild wild mosquito population. It is denoted by $E_u = (A_u^*, 0, F_u^*, 0, M_u^*, 0)^T$, with:

$$A_u^* = K_a\left(1 - \frac{1}{\mathcal{R}_u}\right), \quad F_u^* = b_f \frac{\gamma}{\mu_f} A_u^*, \quad M_u^* = b_m \frac{\gamma}{\mu_m} A_u^*. \tag{15}$$

Thus, the condition $\mathcal{R}_u > 1$ is necessary and sufficient for the existence of E_u.

A_3) ***Microsporidia MB-infected mosquito population only*** The existence and stability of the complete infection equilibrium (CIE) translates the ideal case for the fight against malaria where the population of wild mosquitoes is entirely replaced by a population of mosquitoes carrying *Microsporidia MB* infection. It is obtained by setting $A_u = F_u = M_u = 0$ and we have $E_i = (0, A_i^*, 0, F_i^*, 0, M_i^*)^T$ where,

$$A_i^* = K_a\left(1 - \frac{1}{\mathcal{R}_i}\right), \quad F_i^* = b_f \frac{\gamma}{\mu_f} A_i^*, \quad M_i^* = b_m \frac{\gamma}{\mu_m} A_i^*. \tag{16}$$

Remark 1 The CIE E_i is obtained only in the case of perfect maternal transmission between infected adults (i.e. $\rho_1 = 1$)as we will see shortly later. More precisely, the necessary and sufficient for the existence of E_i are $\mathcal{R}_i > 1$ and $\rho_1 = 1$ is. In the oder hand, when $\rho_1 < 1$, The CIE is replaced by the coexistence equilbrium (CE) where we have both mosquito populations.

Before characterizing this equilibrium point, we define and calculate the basic reproduction number of the model (2).

Computation of the Basic Reproduction Number $\mathcal{R}_0$

The basic reproduction number $\mathcal{R}_0$ for mathematical models in epidemiology provides the threshold condition for which an infection spreads or disappears in the population. $\mathcal{R}_0$ here is interpreted as the average number of wild mosquitoes (males or females) infected vertically or horizontally following the introduction of an infected mosquito. It determines the invasion capacity of wild mosquitoes by infected mosquitoes. We calculate this quantity following the next generation matrix method presented in [25]. For this we collect all the infected mosquito

compartments of the system (2). We pose $X_i = (A_i, F_i, M_i)^T$ and we have:

$$\frac{dX_i}{dt} = \begin{pmatrix} \phi\left[\dfrac{\rho_1 M_i F_i + \rho_2 M_u F_i + \rho_3 \lambda_m M_i F_u}{M_u + M_i}\right]\left(1 - \dfrac{A}{K_a}\right) \\ \beta_m \frac{M_i}{M_u + M_i} F_u \\ \beta_f \frac{F_i}{F_u + F_i} M_u \end{pmatrix} - \begin{pmatrix} (\gamma + \mu_a) A_i \\ -b_f \gamma A_i + \mu_f F_i \\ -b_m \gamma A_i + \mu_m M_i \end{pmatrix}$$
$$=: \mathcal{F} - \mathcal{V}$$

$\mathcal{F}$ represents the flow of newly infected and $\mathcal{V}$ denotes the various transfers between classes due to causes other than infection. The Jacobian matrices of $\mathcal{F}$ and $\mathcal{V}$ at the IFE E_u are given by:

$$J_{\mathcal{F}} = \begin{pmatrix} 0 & \rho_2 \dfrac{\phi}{\mathcal{R}_u} & \rho_3 \lambda_m \dfrac{\phi}{\mathcal{R}_u} \dfrac{b_f \mu_m}{b_m \mu_f} \\ 0 & 0 & \beta_m \dfrac{b_f \mu_m}{b_m \mu_f} \\ 0 & \beta_f \dfrac{b_m \mu_f}{b_f \mu_m} & 0 \end{pmatrix}, \quad J_{\mathcal{V}} = \begin{pmatrix} \gamma + \mu_a & 0 & 0 \\ -b_f \gamma & \mu_f & 0 \\ -b_m \gamma & 0 & \mu_m \end{pmatrix}. \tag{17}$$

The basic reproduction number is the spectral radius of the next generation matrix of the system (2) the matrix $J_{\mathcal{F}} J_{\mathcal{V}}^{-1}$,

$$\mathcal{R}_0 = \frac{1}{2}\left[\rho_2 + \rho_3 \lambda_m + \sqrt{(\rho_2 + \rho_3 \lambda_m)^2 + \frac{4}{\mu_m \mu_f}\left(\rho_2 \mu_m \beta_m + \rho_3 \lambda_m \mu_f \beta_f + \beta_m \beta_f\right)}\right]. \tag{18}$$

Using the notations

$$R_{0v} = \rho_2 + \rho_3 \lambda_m, \quad \text{and} \quad R_{0h} = \frac{1}{\mu_m \mu_f}(\rho_2 \mu_m \beta_m + \rho_3 \lambda_m \mu_f \beta_f + \beta_m \beta_f), \tag{19}$$

the expression of $\mathcal{R}_0$ takes the form:

$$\mathcal{R}_0 = \frac{1}{2}\left[R_{0v} + \sqrt{(R_{0v})^2 + 4R_{0h}}\right]. \tag{20}$$

The definitions of the quantities R_{0v} and R_{0h} are difficult to interpret as breeding numbers. However, R_{0v} reflects the effect of vertical transmission resulting from mating between a wild and an infected mosquito on the ability of infected mosquitoes to invade the wild population. R_{0h} reflects the effect of horizontal transmission of *Microsporidia MB* on the ability of infected mosquitoes to invade the wild population.

Remark 2 The expression that of $\mathcal{R}_0$ independent on the rate of imperfect maternal transmission (ρ_1) between infected adult mosquitoes. This can be justified by the fact that $\mathcal{R}_0$ refers to the average number of secondary infections produced in a population of wild mosquitoes, by an infected mosquito during its entire infectious period [26].

Proposition 2 *Let $\mathcal{T}_0$ be the quantity defined by:*

$$\mathcal{T}_0 = R_{0v} + R_{0h}. \tag{21}$$

Then,

i) $\mathcal{R}_0 > 1$ *if and only if* $\mathcal{T}_0 > 1$,

ii) $\mathcal{R}_0 < 1$ *if and only if* $\mathcal{T}_0 < 1$,
iii) $\mathcal{R}_0 = 1$ *if and only if* $\mathcal{T}_0 = 1$.

$\mathcal{T}_0$ *thus defined is an epidemic threshold in the same way as* $\mathcal{R}_0$.

Proof It is sufficient to note that

$$\begin{aligned}\mathcal{T}_0 - 1 &= R_{0v} + R_{0h} - 1 \\ &= \left(\frac{1}{2}\left(R_{0v} + \sqrt{R_{0v}^2 + 4R_{0h}}\right) - 1\right)\left(1 + \frac{1}{2}\left(\sqrt{R_{0v}^2 + 4R_{0h}} - R_{0v}\right)\right) \\ &= (\mathcal{R}_0 - 1)\left(1 + \frac{1}{2}\left(\sqrt{R_{0v}^2 + 4R_{0h}} - R_{0v}\right)\right).\end{aligned}$$

Since $\sqrt{R_{0v}^2 + 4R_{0h}} - R_{0v} \geq 0$, then $\mathcal{T}_0 - 1$ and $\mathcal{R}_0 - 1$ are of the same sign and we have $\mathcal{T}_0 = 1$ if and only if $\mathcal{R}_0 = 1$. □

A_4) ***Coexistence of mosquito populations*** Since maternal transmission of *Microsporidia MB* infection is naturally imperfect, it is more realistic to consider that $\rho_1 < 1$. In this situation, the complete infection equilibrium point E_i is replaced by the equilibrium point E^c where the two mosquito populations coexist. In this situation, we wish to have a maximum of infected mosquitoes (See Appendix A.1). We define the coexistence equilibrium point as $E^c = (A_u^c, A_i^c, F_u^c, F_i^c, M_u^c, M_i^c)$, with:

$$\begin{aligned}&F_u^c = K_a \frac{b_f \gamma}{\mu_f}\left(1 - \frac{1}{\mathcal{R}_u}\right)\left(\frac{1-p}{1-p+\alpha p}\right), \quad A_u^c = \frac{\beta_m p + \mu_f}{b_f \gamma} F_u^c, \\ &A_i^c = \frac{p}{1-p}\left(\frac{\mu_f \alpha - (1-p)\beta_m}{b_f \gamma}\right) F_u^c, \quad F_i^c = \alpha \frac{p}{1-p} F_u^c, \\ &M_u^c = (1 - p + \alpha p) l F_u^c, \quad M_i^c = \frac{p}{1-p}(1 - p + \alpha p) l F_u^c.\end{aligned} \tag{22}$$

In (22), α and l are giving by

$$\alpha = \frac{\mu_m}{\mu_f}\left(\frac{\beta_m + \mu_f}{\beta_f + \mu_m}\right), \text{ and } l = \frac{b_m \mu_f}{b_f \mu_m},$$

and the parameter p is the proportion of infected males within the total male population at the equilibrium and given by

$$p = \frac{M_i^c}{M_u^c + M_i^c} = \frac{\beta_m - \alpha\mu_f(1 - \rho_2 - \rho_3\lambda_m)}{\beta_m - \alpha\mu_f(\rho_1 - \rho_2 - \rho_3\lambda_m)} \tag{23}$$

Proposition 3 *We assume that* $\rho_1 < 1$ *and* $\frac{\beta_m}{\mu_m}.\frac{\beta_f}{\mu_f} < 1$.
Let $d = 1 + \frac{1}{2}\left(\sqrt{R_{0v}^2 + 4R_{0h}} - R_{0v}\right)$ *and we define the quantity*

$$\mathcal{R}_0^* = 1 - \frac{\rho_3\lambda_m}{d}\left(\frac{\beta_m}{\mu_f} - \frac{\beta_f}{\mu_m}\right). \tag{24}$$

Then, the system (13) admits the point E^c given by (22) as an equilibrium point inside $\mathcal{D}$ if $\mathcal{R}_u > 1$ and $\mathcal{R}_0 > \mathcal{R}_0^*$.

Moreover, the fraction p of infected males in the total population of males at the equilibrium is given by the following expression:

$$p = \frac{\mathcal{R}_0 - \mathcal{R}_0^*}{\mathcal{R}_0 - \mathcal{R}_0^* + \dfrac{1-\rho_1}{d}\left(1 + \dfrac{\beta_m}{\mu_f}\right)}. \tag{25}$$

Proof (Appendix A.2) □

Remark 3 In Proposition 3 above, the quantity $(\beta_m\beta_f)/(\mu_m\mu_f)$ is actually the target reproduction number of (2)when only horizontal transmission is accounted for [27]. The assumption $(\beta_m\beta_f)/(\mu_m\mu_f) < 1$ is not only a mathematical working artefact, rather a condition observed form field from the experiment [18], which highlights the fact that the average number of horizontally infected mosquitoes is less than one.

Stability of Equilibrium Points: Case $\rho_1 = 1$

The stability of an equilibrium point is given by studying the sign of the eigenvalues of the Jacobian matrix of the system (2) evaluated at this point. When maternal transmission between infected adult mosquitoes is perfect ($\rho_1 = 1$), the transmission model (2) admits the points E_u and E_i as equilibrium points distinct from the origin E_0. We have the following result:

Theorem 2 *When maternal infection is perfect ($\rho_1 = 1$), the following statement hold:*

- *The equilibrium point without infection $E_u = (A_u^*, 0, F_u^*, 0, M_u^*, 0)^T$ given by (15) is locally asymptotically stable (LAS) if and only if $\mathcal{R}_u > 1$ and $\mathcal{R}_0 < 1$.*
- *The complete infection equilibrium point $E_i = (0, A_i^*, 0, F_i^*, 0, M_i^*)^T$ given by (16) is locally asymptotically stable (LAS) if and only if $\mathcal{R}_i > 1$ and $\mathcal{R}_0 > 1$.*

Proof (See Appendix B) □

Stability of Equilibrium Points: Case $0 < \rho_1 < 1$

When maternal transmission between infected adult mosquitoes is imperfect ($0 < \rho_1 < 1$), the system (2) admits two equilibrium points distinct from the origin E_0: The infection-free equilibrium point E_u and the coexistence equilibrium point E^c. We have the following results:

Theorem 3 *The equilibrium point $E_u = (A_u^*, 0, F_u^*, 0, M_u^*, 0)^T$ given by (15) is locally asymptotically stable (LAS) if and only if $\mathcal{R}_u > 1$ and $\mathcal{R}_0 < 1$.*

Proof To avoid redundancy, we skip this proof because it is similar to that of Theorem 2. □

Theorem 4 *The coexistence equilibrium point $E^c = (A_u^c, A_i^c, F_u^c, F_i^c, M_u^c, M_i^c)^T$ given by (A10) is locally asymptotically stable (LAS) if $\mathcal{R}_u > 1$ and $\mathcal{R}_0 > 1$. It is unstable for $\mathcal{R}_u > 1$ and $\mathcal{R}_0^* < \mathcal{R}_0 < 1$.*

Table 4 Existence and stability conditions of the equilibrium points

Equilibrium points	Stability conditions (LAS)	
Rate of $M_i \times F_i$ transmission	Case $\rho_1 = 1$	Case $0 < \rho_1 < 1$
Mosquito-free equilibrium (E_0)	$\mathcal{R}_u < 1$ and $\mathcal{R}_i < 1$	$\mathcal{R}_u < 1$ and $\mathcal{R}_i < 1$
Infection-free equilibrium (E_u)	$\mathcal{R}_u > 1$ and $\mathcal{R}_0 < 1$	$\mathcal{R}_u > 1$ and $\mathcal{R}_0 < 1$
Complete infection equilibrium (E_i)	$\mathcal{R}_i > 1$ and $\mathcal{R}_0 > 1$	does not exist
Coexistence equilibrium (E^c)	Does not exist	$\mathcal{R}_u > 1$ and $\mathcal{R}_0 > 1$

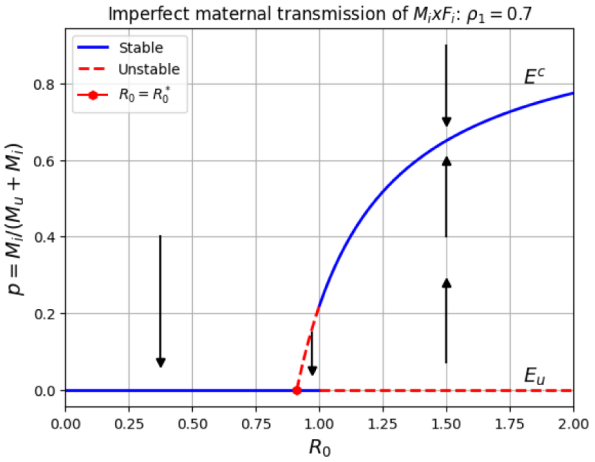

Fig. 4 Bifurcation plot when $\rho_1 < 1$. *This plot shows the stability of equilibrium points as a function of* $\mathcal{R}_0$ *for imperfect maternal transmission between infected adult mosquitoes. The horizontal line represents the stable and unstable states of the equilibrium point* E_u. *The half parabola represents the stable and unstable states of the coexistence equilibrium* E^c *(for* $0 < p < 1$*). The blue lines denote the stable states and the red dashed lines the unstable states. The black arrows indicate the direction of the vector field*

In contrast to the previous cases, computing the Jacobian matrix at the E^c point gives us a full 6×6 matrix whose eigenvalue sign analysis is quite complex. We therefore resort to numerical simulations in order to prove the stability of E^c. The Table 4 summarizes the existence and local stability conditions of the equilibrium points of the system (2).

When $\mathcal{R}_0 < \mathcal{R}_0^*$, The IFE E_u is the only equilibrium point and is globally stable. When $\mathcal{R}_0 > \mathcal{R}_0^*$, we have two equilibria: In the interval $\mathcal{R}_0^* < \mathcal{R}_0 < 1$, the equilibrium E_u is stable and E^c is unstable; in the interval $\mathcal{R}_0 > 1$ the equilibrium E_u is unstable and E^c is stable For our simulation, the point $\mathcal{R}_0 = \mathcal{R}_0^*$ is the threshold condition beyond which we have coexistence of both mosquito populations (Fig. 4).

Time Evolution of Mosquito Populations in Different Scenarios

Figure 5a reflects the extinction case for both groups of mosquitoes. Figure 5b reflects the case of complete infection where wild mosquitoes are totally replaced by infected mosquitoes as soon as $\mathcal{R}_0 > 1$, whatever the small proportion of infected mosquitoes introduced at the beginning. Figure 5c shows the situation where the population of infected mosquitoes eventually disappears (IFE) as soon as $\mathcal{R}_0 < 1$.

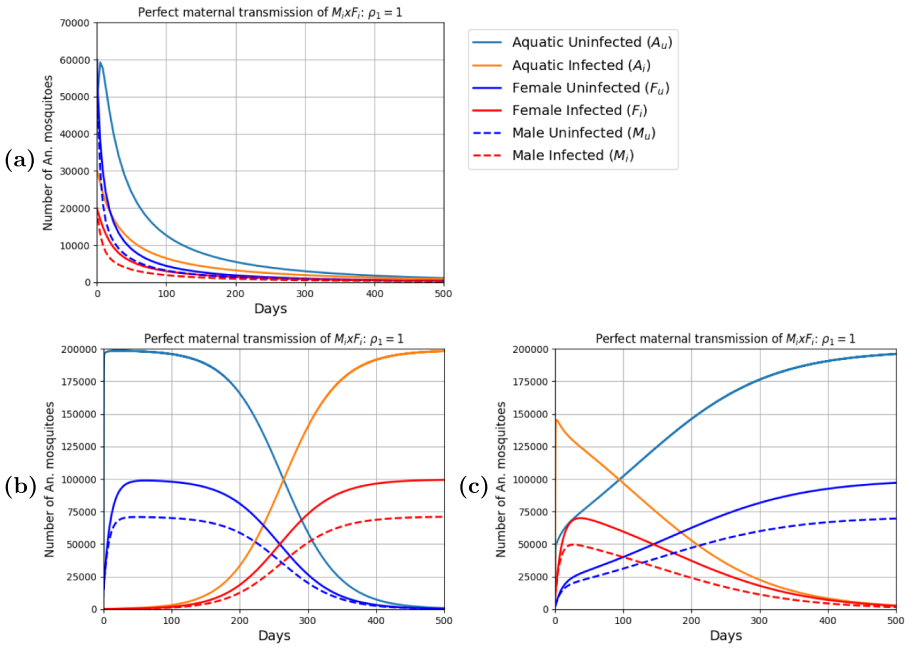

Fig. 5 Perfect maternal transmission between infected adult mosquitoes. **a** *Represents the case of extinction of both populations*, $\mathcal{R}_u = \mathcal{R}_u = 0.77$, with initial conditions $A_u(0) = 40000$, $A_i(0) = 30000$, $F_u(0) = 60000$, $F_i(0) = 20000$, $M_u(0) = 60000$, *and* $M_i(0) = 20000$. **(b)** *Here*, $\mathcal{R}_0 = 1.42$, $\mathcal{R}_u = \mathcal{R}_i = 240$, *with initial conditions* $A_u(0) = 10000$, $A_i(0) = 20$, $F_u(0) = 15000$, $F_i(0) = 0$, $M_u(0) = 15000$, *and* $M_i(0) = 20$. **(c)** *We have* $\mathcal{R}_0 = 0.85$, $\mathcal{R}_u = \mathcal{R}_i = 200$, *with initial conditions* $A_u(0) = 4000$, $A_i(0) = 4000$, $F_u(0) = 2000$, $F_i(0) = 10000$, $M_u(0) = 2000$, *and* $M_i(0) = 10000$

Figure 6 allows us to justify Theorem 4. Indeed in the both situation, we have $\mathcal{R}_0 > \mathcal{R}_0^*$ and thus the coexistence of the two mosquito populations corresponding to the point E^c. We observe that for $\mathcal{R}_0 > 1$, the curves translating the density of the mosquito population tend towards this point and therefore it is stable. In this case, $\mathcal{R}_0 < 1$ and the mosquito population density curves move away from the equilibrium point, so it is unstable.

The Full Sex-Structured Model Versus Its Reduced Counterparts

In this section, we assess the accuracy of our model reduction process by comparing the reproduction numbers and threshold conditions for infection establishment between the full model and reduced models. In this regards, we will refer to full sex-structured model as **6-ODE model**, to the reduced four-dimensional system as **4-ODE model**, and to the reduced two-dimensional system as **2-ODE model**.

Comparison of the Reproduction Numbers and Equilibrium Points

The 4-ODE Model

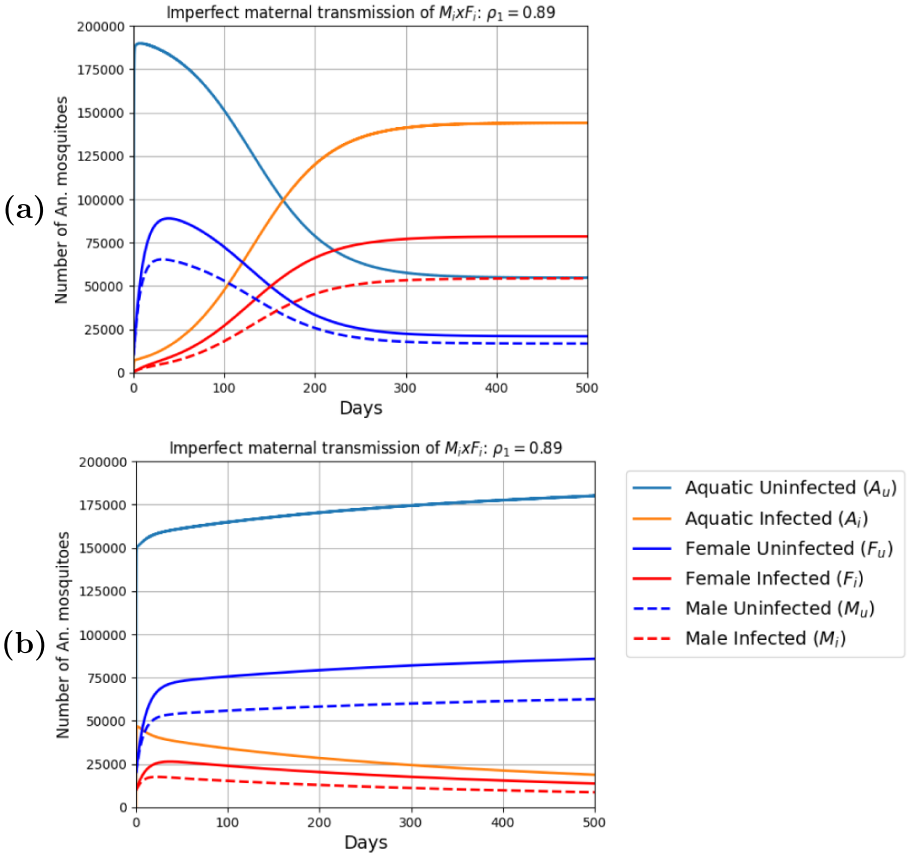

Fig. 6 Coexistence of the both populations. *In (a) we have*: $\mathcal{R}_0 = 1.37$, $\mathcal{R}_0^* = 0.95$, $\mathcal{R}_u = 200$ *and* $\mathcal{R}_i = 140$, *with initial conditions* $A_u(0) = 5000$, $A_i(0) = 0$, $F_u(0) = 10000$, $F_i(0) = 500$, $M_u(0) = 10000$, *and* $M_i(0) = 500$. *In the simulation (b),* $\mathcal{R}_0 = 0.97$, $\mathcal{R}_0^* = 0.94$, $\mathcal{R}_u = 285.71$ *and* $\mathcal{R}_i = 254$, *with initial conditions* $A_u(0) = 10000$, $A_i(0) = 0$, $F_u(0) = 20000$, $F_i(0) = 12000$, $M_u(0) = 20000$, *and* $M_i(0) = 12000$

In the 4-ODE model, the reproduction numbers for the population of wild mosquitoes ($\mathcal{R}_u^{(4)}$) and infected mosquitoes ($\mathcal{R}_i^{(4)}$) are given by:

$$\mathcal{R}_u^{(4)} = b_f \frac{\phi_i'}{\mu_f} = b_f \frac{\gamma}{\gamma + \mu_a} \frac{\phi}{\mu_f} = \mathcal{R}_u, \tag{26}$$

$$\mathcal{R}_i^{(4)} = \rho_1 b_f \frac{\phi_i'}{\mu_f} = \rho_1 b_f \frac{\gamma}{\gamma + \mu_a} \frac{\phi}{\mu_f} = \mathcal{R}_i. \tag{27}$$

The 4-ODE model exhibits three equilibrium points under certain conditions:

- Mosquito-free equilibrium (MFE): $E_0^{(4)} = (0, 0, 0, 0)^T$.
- Infection-free equilibrium (IFE): $E_u^{(4)} = (F_u^*, 0, M_u^*, 0)^T$.

- Complete infection equilibrium (CIE): $E_i^{(4)} = (0, F_i^*, 0, M_i^*)^T$, where

$$F_\sigma^* = K\left(1 - \frac{1}{\mathcal{R}_\sigma^{(4)}}\right), \quad M_\sigma^* = rK\left(1 - \frac{1}{\mathcal{R}_\sigma^{(4)}}\right), \tag{28}$$

with $\sigma \in \{u, i\}$.

When the maternal transmission between infected mosquitoes is imperfect ($\rho_1 < 1$) and $\mathcal{R}_u^{(4)} > 1$, the complete infection equilibrium (CIE) is replaced by the coexistence equilibrium (CE) given by $E_c^{(4)} = (F_u^c, F_i^c, M_u^c, M_i^c)^T$, where:

$$\begin{aligned} F_u^c &= K\left(1 - \frac{1}{\mathcal{R}_u^{(4)}}\right)\left(\frac{1-p}{1-p+\alpha p}\right), \quad F_i^c = \alpha\frac{p}{1-p}F_u^c, \\ M_u^c &= (1-p+\alpha p)lF_u^c, \quad M_i^c = \frac{p}{1-p}(1-p+\alpha p)lF_u^c. \end{aligned} \tag{29}$$

The parameters α, p and l are those given in (22).

To determine the basic reproduction number ($\mathcal{R}_0^{(4)}$) of the 4-ODE system, we utilize the next generation matrix method [25], which yields:

$$\mathcal{R}_0^{(4)} = \frac{1}{2}\left(R_{0v} + \sqrt{(R_{0v})^2 + 4R_{0h}}\right), \tag{30}$$

where R_{0v} and R_{0h} are given by (19). Thus, the basic reproduction number for the reduced 4-dimensional model is exactly the same as that of the 6-ODE model. Hence, the reduction process leading to the four-dimensional system did preserve the main epidemiological threshold for the population dynamics of mosquitoes.

The 2-ODE Model

In the 2-ODE model, the reproduction numbers for the population of wild mosquitoes ($\mathcal{R}_u^{(2)}$) and infected mosquitoes ($\mathcal{R}_i^{(2)}$) are given by:

$$\mathcal{R}_u^{(2)} = \frac{b}{\mu_f} = b_f\frac{\gamma}{\gamma+\mu_a}\frac{\phi}{\mu_f} = \mathcal{R}_u, \tag{31}$$

$$\mathcal{R}_i^{(2)} = \rho_1\frac{b}{\mu_f} = \rho_1 b_f\frac{\gamma}{\gamma+\mu_a}\frac{\phi}{\mu_f} = \mathcal{R}_i. \tag{32}$$

The 2-ODE model exhibits three equilibrium points under certain conditions:

- Mosquito-free equilibrium (MFE): $E_0^{(2)} = (0, 0)$.
- Infection-free equilibrium (IFE): $E_u^{(2)} = (F_u^*, 0)$.
- Complete infection equilibrium (CIE): $E_i^{(2)} = (0, F_i^*)$, where

$$F_\sigma^* = K\left(1 - \frac{1}{\mathcal{R}_\sigma^{(2)}}\right), \text{ with } \sigma \in \{u, i\}. \tag{33}$$

When the maternal transmission between infected mosquitoes is imperfect ($\rho_1 < 1$) and $\mathcal{R}_u^{(2)} > 1$, the complete infection equilibrium (CIE) is replaced by the coexistence equilibrium (CE) given by:

$$E_c^{(2)} = (F_u^c, F_i^c), \tag{34}$$

Table 5 Sensitivity analysis of the full and reduced model *Comparison of the local sensitivity indices of the general model and the reduced model for the base values of the variables v in Table 2*

w = Basic reproduction number		
v	**6-ODE/4-ODE**	**2-ODE**
ρ_2	0.546	0.529
ρ_3	0.207	0.206
λ	0.217	0.219
β	0.312	0.331
μ_f	−0.311	−0.330
Basic reproduction number for baseline value		
$\mathcal{R}_0 = \mathcal{R}_0^{(4)} = 0.96$		$\mathcal{R}_0^{(2)} = 0.97$

where

$$F_u^c = (1 - p_f)K\left(1 - \frac{1}{\mathcal{R}_u^{(2)}}\right), \quad F_i^c = \frac{p_f}{1 - p_f}F_u^c, \tag{35}$$

and the quantity p_f is defined as:

$$p_f = \frac{\mathcal{R}_0^{(2)} - 1}{\mathcal{R}_0^{(2)} - \rho_1}. \tag{36}$$

Here, p_f represents the proportion of infected females.

To calculate the basic reproduction number ($\mathcal{R}_0^{(2)}$) of the 2-ODE system in equation (11), we employ the next generation matrix method [25], resulting in:

$$\mathcal{R}_0^{(2)} = \rho_2 + \rho_3\lambda + \frac{\beta}{\mu_f}. \tag{37}$$

It is worth noticing that when $\mu_m = \mu_f$ and $\beta_m = \beta_f$, we have $\mathcal{R}_0 = \mathcal{R}_0^{(2)}$. However, the following gives the values of the three basic reproduction numbers obtained throughout the reduction processes, when the baseline parameter values are used.

Analysis of the Sensitivity of the Models

The analysis of the sensitivity displayed in Table 5 consists in examining how the key parameters of invasion of *Microsporidia MB* in the full model and in the reduced model vary according to the disturbances carried out on the values of the parameters of each model given in Table 2 of "Model Formulation" section.

Definition 1 The normalized direct sensitivity index of w with respect to a parameter v is defined by:

$$S_v^w = \frac{v}{w} \times \frac{\partial w}{\partial v}. \tag{38}$$

It measures the variation of the output variable w as a function of the input variable v. More precisely, if v grows by $x\%$ then w grows by $S_v^w \times x\%$

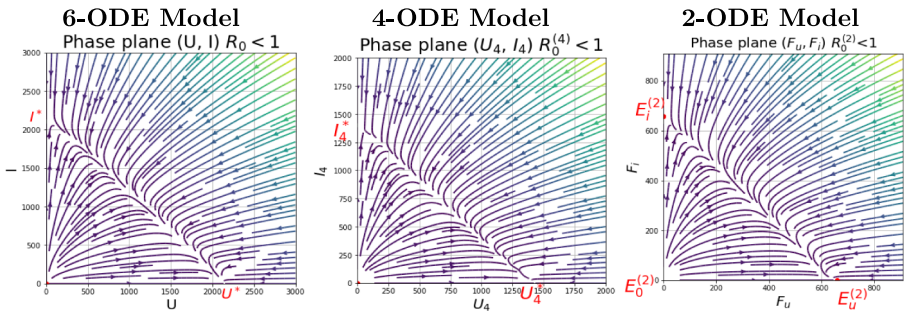

Fig. 7 Global asymptotic stability (GAS) of IFE

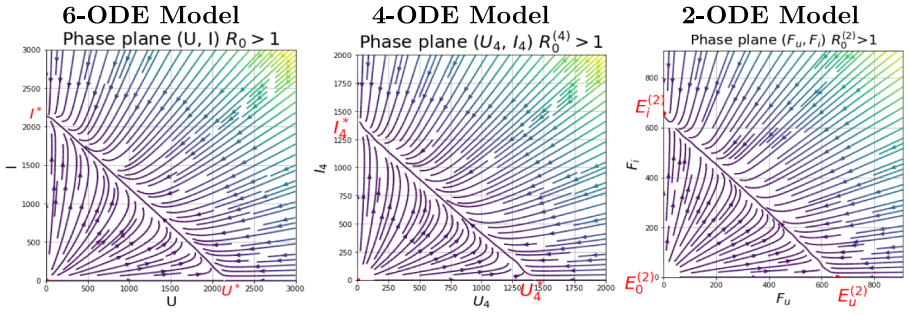

Fig. 8 Global asymptotic stability (GAS) of CIE

Comparison of Asymptotic Behavior: Phase Portraits

In this section, we perform a comprehensive analysis of equilibrium stability in both the original and reduced models, with a focus on the phase plane dynamics. We investigate the influence of the basic reproduction number on equilibrium stability and compare the results across different model configurations.

To facilitate our analysis, we introduce the following quantities: $U = A_u + F_u + M_u$, $I = A_i + F_i + M_i$, $U_4 = F_u + M_u$, and $I_4 = F_i + M_i$. These variables represent the population levels of susceptible and infected individuals in the 6-EDO model and the 4-EDO model.

Perfect Maternal Transmission ($\rho_1 = 1$): We first explore the stability of equilibrium points in the context of perfect maternal transmission, where the maternal transmission rate ρ_1 equals unity. Our investigations encompass both the original models and their reduced counterparts.

Remarkably, throughout our analysis, we maintain the integrity of the equilibria and their stability properties. Figure 7 demonstrates the global asymptotic stability (GAS) of the Infection-Free Equilibrium (IFE) when the basic reproduction number falls below unity, while Fig. 8 showcases the GAS of the Chronic Infection Equilibrium (CIE) for basic reproduction numbers exceeding unity.

Imperfect Maternal Transmission ($\rho_1 < 1$): Next, we extend our investigation to account for imperfect maternal transmission, where the maternal transmission rate ρ_1 is less than one. Similar to the previous scenario, we meticulously preserve the number of equilibria and their stability characteristics when reducing the model complexity.

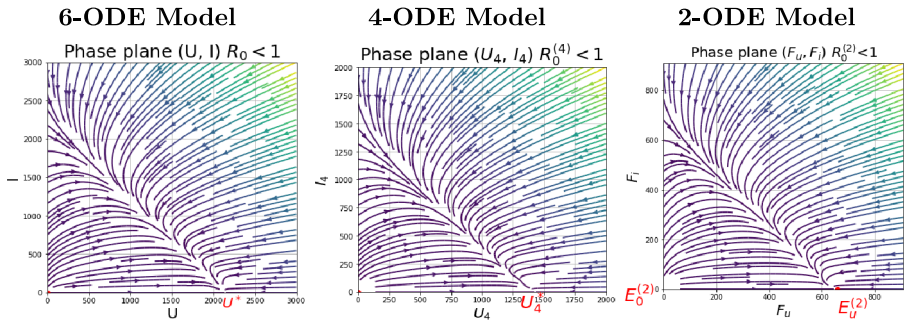

Fig. 9 Global asymptotic stability (GAS) of IFE

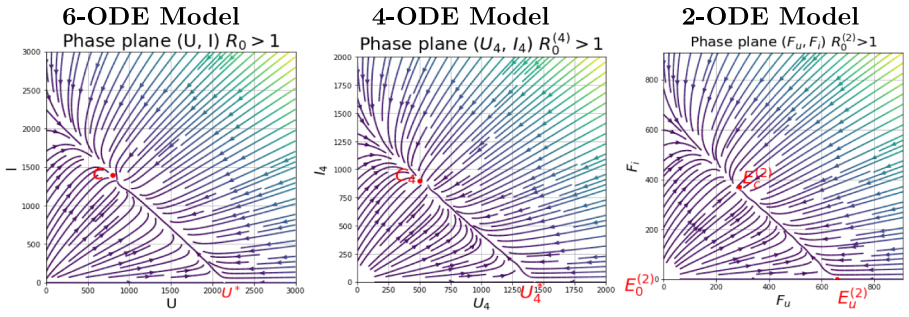

Fig. 10 Global asymptotic stability (GAS) of CIE

Figure 9 showcases the global stability of the IFE when the basic reproduction number is less than one, while Fig. 10 presents the stability of the CIE for basic reproduction numbers greater than one.

Comparison of the Invasion Frequency

One of the key assumptions in the model reduction process is the rapid development of aquatic mosquitoes into adults. As shown in the following figure, when the maturation rate into adults (γ) is high, the progression of Microsporidia MB infection in both the general model and the reduced model is almost identical.

The Figs. 11, 12 show the evolution of the proportion of infected females in the two models over time for different values of the rate of maturation in the aquatic stage. The upper curves (in red) in each of the graphs represent the case of invasion of *Microsporidia MB* and the lower curves (in purple) reflect the case of disappearance of the infection with *Microsporidia MB*. With an initial infection rate of 33% for cases $\rho_1 = 1$ and 42% for cases $\rho_1 < 1$.

The reduced model describes the dynamics of transmission of the infection within the population of females for a rapid hatching rate and a high maturation of mosquitoes at the aquatic stage into adults as well as a mortality rate of males and females. relatively close. The model obtained has the advantage of being able to characterize the basins of attraction of the equilibrium points and more simplistic stability conditions. Since *Microsporidia MB* infection is at a very low level in nature, it is therefore necessary to introduce infected

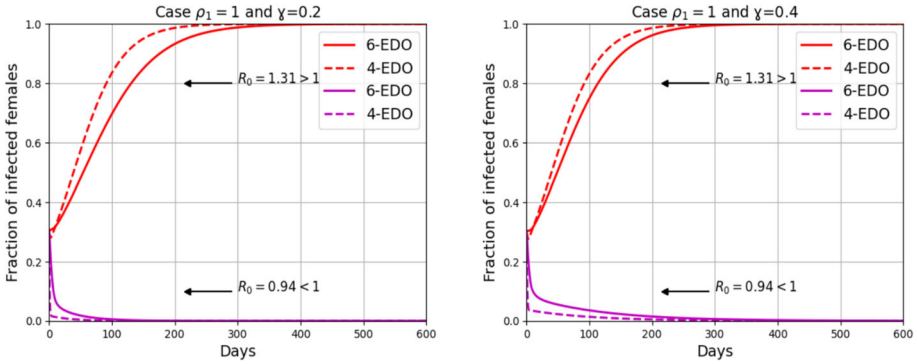

Fig. 11 Comparison of **6-ODE** and **4-ODE**

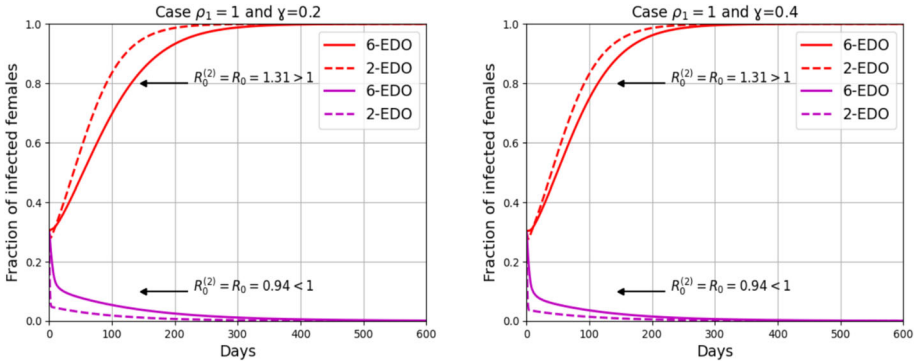

Fig. 12 Comparison of **6-ODE** and **2-ODE**

mosquitoes into nature. In the next chapter we will study the different control strategies that can be used to ensure that wild mosquitoes are replaced by infected mosquitoes.

Mosquito Release Strategies

Microsporidia MB infection is present at relatively low prevalence in the Anopheles mosquito population [17], suggesting that $\mathcal{R}_0 < 1$. In fact, for the baseline values, the basic reproduction number of our model is $\mathcal{R}_0 \approx 0.96$. This value does not insure the natural persistence of MB-infected mosquitoes in the population. Therefore, an attempt to reverse this undesired situation is to design and implement some classical control strategies consisting in releasing laboratory MB-infected rearing mosquitoes in the wild mosquito population [12]. Typically, in this regards, there are many release methods and for the seek of simplicity, we shall consider only two continuous possible release strategies as presented below.

1. **Continuous releases with constant release rate**: In this case, we release a constant number of mosquitoes carrying *Microsporidia MB* infection cultured in the laboratory.
2. **Continuous releases with variable release rate**: In this case, the release rate of infected mosquitoes is a function of time.

Based on the hierarchical reduction approach, we can implement various control strategies on the reduced 2-ODE model for the transmission of the infection, specifically targeting *Microsporidia MB*. This involves the introduction of infected mosquitoes when the value of $\mathcal{R}_0^{(2)}$ exceeds 1 (approximately 0.97 for the baseline parameter values).

Releases with Constant Rate

In order to model these releases, we introduce into the reduced model the variable **r**, the (constant) release rate of mosquitoes. The rate **r** expresses the fraction of mosquitoes infected with *Microsporidia MB* released each day as a percentage of infected mosquitoes present in the locality on the same day [12]. The fitted model takes the form:

$$\begin{cases} \dfrac{dF_u}{dt} = b\left(\dfrac{F_u^2 + (1-\rho_1)F_i^2 + (1-\rho_2)F_uF_i + (1-\rho_3\lambda)F_iF_u}{F_u+F_i}\right)\left(1-\dfrac{F_u+F_i}{K}\right) \\ \qquad\qquad -\beta\dfrac{F_i}{F_u+F_i}F_u - \mu_f F_u, \\ \dfrac{dF_i}{dt} = b\left(\dfrac{\rho_1 F_i^2 + \rho_2 F_uF_i + \rho_3\lambda F_iF_u}{F_u+F_i}\right)\left(1-\dfrac{F_u+F_i}{K}\right) \\ \qquad\qquad +\beta\dfrac{F_i}{F_u+F_i}F_u - \mu_f F_i + \mathbf{r}F_i. \end{cases} \tag{39}$$

We associate to the system (39) the initial condition:

$$F_u(0) = K\left(1-\frac{\mu_f}{b}\right), \quad F_i(0) = \mathbf{r}F_u(0). \tag{40}$$

The rate $\mathbf{r} \in [0, \mu_f[$ and is expressed in day^{-1}.

Control Strategies: Case $\rho_1 = 1$

In this situation, the objective of the mosquito release strategy is the total replacement of the wild mosquito population with infected mosquitoes. The analysis of the reduced model assures us of the existence of the complete infection equilibrium point (CIE) which is stable for $\mathcal{R}_0^{(2)} > 1$.

Using the next generation matrix [25] method, we get the base reproduction number of the system (39) given by:

$$\mathbb{G}_0^{\mathbf{r}} = \rho_2 + \rho_3\lambda + \frac{\beta}{\mu_f - \mathbf{r}}. \tag{41}$$

In the absence of control ($\mathbf{r} = 0$), the basic reproduction number is $\mathbb{G}_0^0 = \mathcal{R}_0^{(2)} < 1$. The release rate **r** must therefore be chosen so that $\mathbb{G}_0^{\mathbf{r}} > 1$, leads us to the following condition:

$$\mu_f - \frac{\beta}{1-\rho_2-\rho_3\lambda} < \mathbf{r} < \mu_f \tag{42}$$

Using the baseline values from Table 2, we obtain $0.012 \leq \mathbf{r} < 0.1$.

Figure 13 shows some possible release options. Mosquito releases over a fixed period of time require a large release rate to be efficient in contrast to the case where infected mosquitoes are released indefinitely. This shows that the strategy based on a constant release

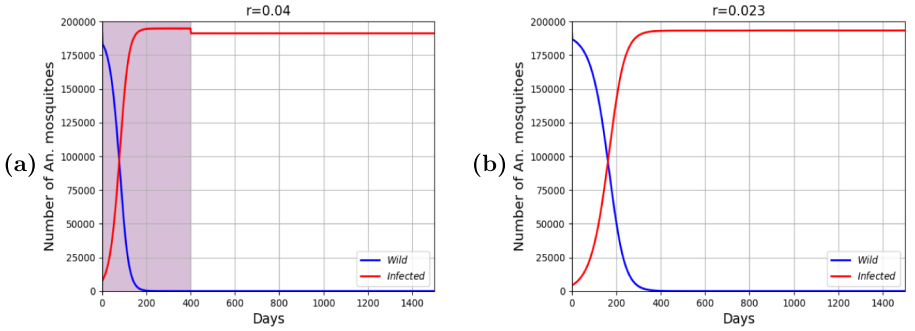

Fig. 13 Constant release strategy of infected mosquitoes when $\rho_1 = 1$ *The purple band in (a) represents the release period of infected mosquitoes with* $t = 400$ *days. In (b) uninterrupted releases over the duration of the experiment are assumed. The blue curves represent the progression of wild mosquitoes and the red curves the progression of infected mosquitoes. We use the following values in the simulation:* $K = 200000$, $b = 2.22$. *The other parameters are taken at their baseline values in Table 2*

rate achieves the replacement of the population, but requires an uninterrupted production of infected mosquitoes in the laboratories, which can be very costly.

Control Strategies: Case $\rho_1 < 1$

For this case, it is no longer possible to achieve total replacement of the wild mosquito population with mosquitoes carrying the *Microsporidia MB*. infection. According to the analysis made in the previous sections, it is possible to have the coexistence of the both mosquito populations which is stable for $\mathcal{R}_0^{(2)} > 1$. The aim of this release strategy is to considerably reduce the size of the wild mosquito population.

In the absence of control, the proportion of infected mosquitoes at the coexistence equilibrium is given by:

$$p_f = \frac{\mathcal{R}_0^{(2)} - 1}{\mathcal{R}_0^{(2)} - \rho_1}.$$

The objective is to have a higher number of infected mosquitoes than wild mosquitoes ($p_f > 0.5$ or $\mathcal{R}_0^{(2)} > 2 - \rho_1$). We then choose $\mathbf{r}$ such that $\mathbb{G}_0^{\mathbf{r}} > \mathcal{R}_0^{(2)} > 2 - \rho_1$. This leads to

$$\mu_f - \frac{\beta}{2 - \rho_1 - \rho_2 - \rho_3\lambda} < \mathbf{r} < \mu_f. \tag{43}$$

Using the baseline values from Table 2 we get $0.046 \leq \mathbf{r} < 0.1$.

The numerical simulations in Fig. 14 show us some possible release options. This strategy requires a large number of mosquitoes in the releases ($\mathbf{r} \geq 0.046$) in contrast to the $\rho_1 = 1$. Figure 14a and b show that releases effected over limited durations are not efficient regardless of the rate of release of infectioed mosquitoes because wild mosquitoes will take over once releases are stopped. Thus, to achieve the fixed objective it is necessary to release infected mosquitoes uninterruptedly (Fig. 14c, d). In this case the prevalence of the infection will increase according to the importance of the rate of releases carried out.

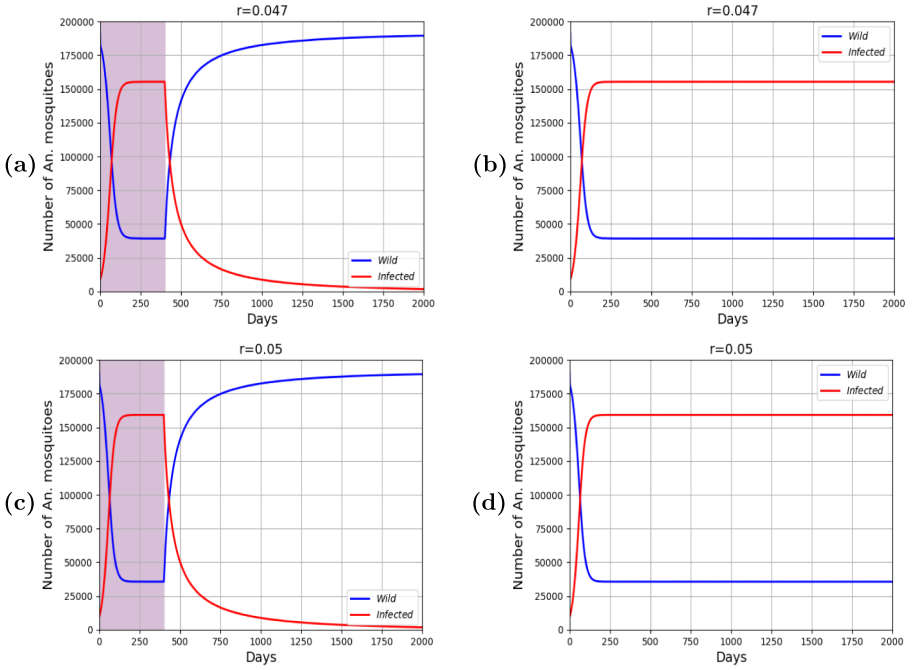

Fig. 14 Constant release strategy of infected mosquitoes when $\rho_1 < 1$ *The purple bands, in (a) and (b) represent the release period of infected mosquitoes. In (c) and (d), uninterrupted releases over the duration of the experiment are assumed. The blue curves represent the progression of wild mosquitoes and the red curves represent the progression of infected mosquitoes. We use in the simulations the values* $K = 200000, b = 2.22,$ $\beta = 0.032, \lambda = 0.51,$ *the other parameters taken at their baseline values in Table 2*

Releases with Variable Rate

For this type of release, similar to the approach in [4, 12, 28], we introduce the control variable $r(t) \in [0, r_{\max}]$, $r_{max} < \mu_f$. is assumed to be continuous (or piecewise continuous) and expresses the time-dependent rate of released infected mosquitoes.

The control model is therefore as follows:

$$\begin{cases} \dfrac{dF_u}{dt} = b\left(\dfrac{F_u^2 + (1-\rho_1)F_i^2 + (1-\rho_2)F_uF_i + (1-\rho_3\lambda)F_iF_u}{F_u+F_i}\right)\left(1-\dfrac{F_u+F_i}{K}\right) \\ \qquad\qquad -\beta\dfrac{F_i}{F_u+F_i}F_u - \mu_f F_u, \\ \dfrac{dF_i}{dt} = b\left(\dfrac{\rho_1 F_i^2 + \rho_2 F_uF_i + \rho_3\lambda F_iF_u}{F_u+F_i}\right)\left(1-\dfrac{F_u+F_i}{K}\right) \\ \qquad\qquad +\beta\dfrac{F_i}{F_u+F_i}F_u - \mu_f F_i + r(t)F_i. \end{cases} \tag{44}$$

With the initial condition:

$$F_u(0) = F_u^0 > 0, \quad F_i(0) = F_i^0 \geq 0. \tag{45}$$

To the system (44), we associate the objective (cost) function

$$\mathcal{J}(r) = F_u^2(T) + \int_0^T Cr^2(t)F_i(t)dt. \tag{46}$$

Where $F_u^2(T)$ is the objective with respect to the population level of wild mosquitoes that we wish to minimize at the final position. Then, our goal is to determine the release rate r^* that minimizes the cost r^* $\mathcal{J}(r)$ at time horizon $[0, T]$ on Γ.

$$\mathcal{J}(r^*) = \min_{r\in\Gamma} \mathcal{J}(r), \tag{47}$$

where

$$\Gamma = \left\{ r \in C^0([0, T]), \ \text{ piecewise } : r(t) \in [0, r_{\max}] \right\}, \tag{48}$$

is the set of admissible controls. $C > 0$ expresses the cost per unit time associated with the release strategy (laboratory production of mosquitoes and releases).

Theorem 5 *Consider the optimal control problem associated with the system (44). There exists a control r^* and a corresponding solution $X^* = (F_u^*, F_i^*)$ which minimizes the functional $\mathcal{J}$ on Γ.*

Proof Since the function $g \equiv F_u^2(T)$ is continuous, to establish the existence of an optimal control, we verify that the conditions of Fleming and Rishel's theorem [29] are satisfied:

1. The set of controls and the set of corresponding solutions is non empty.
2. The set of controls Γ is convex and closed in $L^2([0, T])$.
3. The right part of the Eq. (44) is bounded by a linear function of the control.
4. The integrant of the objective function is convex on Γ and bounded by $a_1|r|^\alpha - a_2$, where $a_1, a_2 > 0$ and $\alpha > 1$.

The condition 1 is obtained thanks to the results of Lukes [30] for systems with constant coefficients. The set Γ is a closed convex set of $L^2(0, T)$ by definition and the right part of the system (44) satisfies the condition 3 because the state variables are bounded. It is clear that the integrant $Cr^2F_i(t)$ of the objective function is convex with respect to r, moreover there exist $a_1, a_2 > 0$ and $\alpha > 1$ such that:

$$Cr^2F_i(t) \geq a_1|r|^\alpha - a_2,$$

because the state variables are bounded. We conclude that there exists an optimal control r^* which minimizes the functional $\mathcal{J}$ on Γ. □

The existence of an optimal control having been established, we are now interested in its characterization. Following [31], we define the Hamiltonian associated with the problem (44)-(46) as:

$$\begin{aligned}\mathcal{H}(F_u, F_i, r, \lambda_1, \lambda_2) &= C_2r^2F_i - \lambda_1.\left(\beta\frac{F_i}{F_u+F_i}F_u + \mu_f F_u\right)\\ &+\lambda_1.\left(\frac{b(F_u^2 + (1-\rho_1)F_i^2 + (1-\rho_2)F_uF_i + (1-\rho_3\lambda)F_iF_u)}{F_u+F_i}\right)\left(1 - \frac{F_u+F_i}{K}\right)\\ &+\lambda_2.\left[\frac{b(\rho_1F_i^2 + \rho_2F_uF_i + \rho_3\lambda F_iF_u)}{F_u+F_i}\left(1-\frac{F_u+F_i}{K}\right) + \beta\frac{F_i}{F_u+F_i}F_u - \mu_f F_i + rF_i\right].\end{aligned} \tag{49}$$

λ_1 and λ_2 are called adjoint variables.

Theorem 6 *Let r^* be an optimal control and $X^* = (F_u^*, F_i^*)$ the corresponding solution. Then there exist adjoint variables $\lambda_1(t)$ and $\lambda_2(t)$ Then there exist adjoint variables verifying the transversality conditions:*

$$\lambda_1(T) = 2F_u(T), \quad \lambda_2(T) = 0. \tag{50}$$

Moreover, the following characterization is verified

$$r^*(t) = \min\left\{\max\left\{0, -\frac{\lambda_2(t)}{2C}\right\}, r_{\max}\right\}. \tag{51}$$

Proof By application of Pontryagin's maximum principle [32], the optimality condition gives us the existence of λ_1 and λ_2 verifying the following adjoint system:

$$\begin{cases} \dfrac{\partial \lambda_1}{\partial t} = -\dfrac{\partial \mathcal{H}}{\partial F_u}, \\ \dfrac{\partial \lambda_2}{\partial t} = -\dfrac{\partial \mathcal{H}}{\partial F_i}. \end{cases} \tag{52}$$

with final time conditions:

$$\lambda_1(T) = \left.\frac{\partial g}{\partial F_u}\right|_{t=T} = 2F_u(T), \quad \lambda_2(T) = 0.$$

– The minimality condition on the set $\{t \in [0, T] : 0 < r^*(t) < r_{\max}\}$ is:

$$\frac{\partial \mathcal{H}}{\partial r^*} = 2r^* C F_i + \lambda_2 F_i = 0.$$

Thus on this set, $r^* = -\dfrac{\lambda_2}{2C}$.

– If $t \in \{t \in [0, T] : r^* = 0\}$, then the minimality condition is:

$$\frac{\partial \mathcal{H}}{\partial r^*} = 2r^* C F_i + \lambda_2 F_i < 0, \quad i.e., \quad -\frac{\lambda_2}{2C} > 0.$$

– If $t \in \{t \in [0, T] : r^* = r_{\max}\}$, then the minimality condition is

$$\frac{\partial \mathcal{H}}{\partial r^*} = 2r^* C F_i + \lambda_2 F_i > 0, \quad i.e., \quad -\frac{\lambda_2}{2C} < r_{\max}.$$

Therefore, we obtain the desired control characterization given by (51) □

Numerical Implementation: Optimal Release

In this section, we are interested in the numerical solution of the optimal release control problem. We have proved in Theorem 5, the existence of an optimal control and an associated optimal solution. We have also given the characterization of the optimal control in Theorems 6 as a function of the level of maternal transmission. In what follows, we use the Python's **gekko** package [33] to solve optimal control problems in order to illustrate these results.

We consider in our numerical simulations that the maximum release rate of infected mosquitoes is $r_{\max} = 0.06$ and we take $C = 1$. The maximum female carrying capacity K is fixed at 20000. We assume that at time $t = 0$, we have $F_u^0 = 15000$ and $F_i^0 = 0.052F_u^0$ i.e. the infected mosquitoes constitute 5% of the total mosquito population at the time of the study. The releases are made over a period of $T = 500$ days and the parameter values used are the same as those for the constant rate releases.

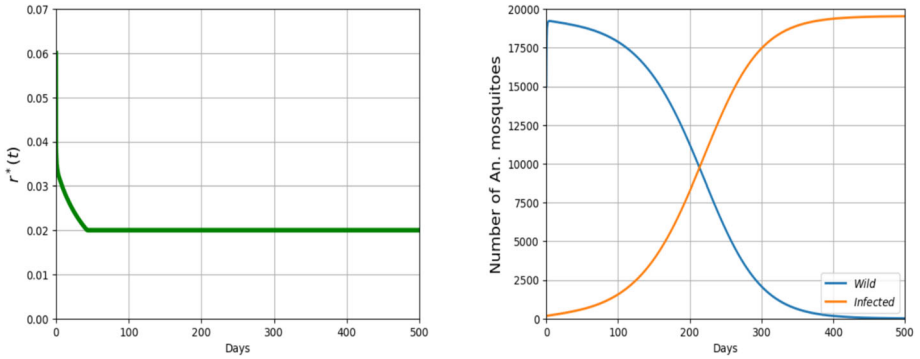

Fig. 15 Optimal release over a 500 day period when $\rho_1 = 1$

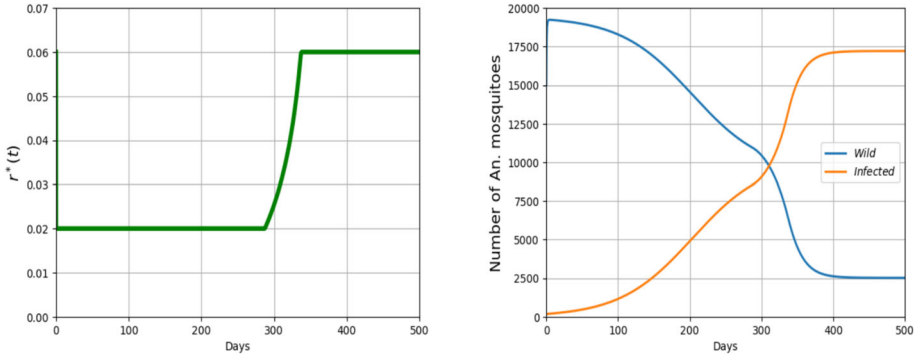

Fig. 16 Optimal release over a 500 day period when $\rho_1 = 0.76 < 1$

Figures 15 and 16 show us the effet control on the growth of the two mosquito populations in the case $\rho_1 = 1$ where population replacement is achieved. Figure 16 reflects the case of coexistence of the both populations ($\rho_1 < 1$) where the objective is to minimize the population density of wild mosquitoes in the final state. The profils of the control are given by the curves in green. At the onset ($t = 0$), the release rate $r^*(t)$ is set to its maximum value ($r_{\max} = 0.06$) to introduce a substantial number of infected mosquitoes into the environment. This initial surge aims to disrupt the existing population dynamics and establish a foundation for the infected group. As the infected mosquitoes integrate and begin to influence the wild population, the efficiency of maternal transmission directly impacts $r^*(t)$. With perfect maternal transmission ($\rho_1 = 1$), the release rate gradually reduces over time as the infected population becomes self-sustaining. Conversely, with imperfect maternal transmission ($\rho_1 < 1$), a more aggressive and sustained release strategy is required to achieve the desired population dynamics.

Discussion and Conclusion

In this study, we have presented a comprehensive mathematical model that explores the interactive dynamics between wild mosquitoes and *Microsporidia MB*-infected mosquitoes. Through rigorous analysis and investigation, we have gained valuable insights into the spread of the infection and its dependence on various factors. Our model allows for a detailed

examination of the population dynamics, considering both the wild and infected mosquito populations. By reducing the full model to smaller, mathematically tractable systems, we have preserved the qualitative and quantitative dynamics, enabling a deeper understanding of the underlying mechanisms at play. One of the key findings of our study is the critical role played by the level of maternal transmission in the successful spread of *Microsporidia MB* infection. Specifically, we have observed that under perfect maternal transmission, population replacement becomes possible, leading to the dominance of infected mosquitoes within the population. Analysis of this model allowed us to determine the threshold conditions on basal reproduction rate for which *Microsporidia MB* the infection persists in the mosquito population ($\mathcal{R}_0 > 1$) with the stability of the CIE. However, when maternal transmission is imperfect, population replacement is no longer attainable. Nevertheless, we have identified that a sufficiently high rate of maternal transmission can still achieve a significant level of infection, with at least 50% of mosquitoes becoming infected, surpassing the minimum target of 40% infection.

We have explored the impact of release rates of infected mosquitoes on population replacement. Our findings indicate that maintaining a release rate that ensures at least 50% population replacement is essential for successful spread. However, we have also discovered that constant releases over a fixed period do not lead to population replacement or the dominance of MB-infected mosquitoes. Instead, employing time-dependent release strategies proves to be more effective in achieving population replacement within a specified timeframe. These results build upon prior studies that have examined the use of release strategies with symbiotic microorganisms like *Wolbachia* for mosquito control [11, 12], highlighting the importance of timing and adaptation in control strategies.

It is important to note that the potential for *Microsporidia MB*-based interventions will depend on various contextual factors. In developed countries with well-established healthcare systems and efficient mosquito control infrastructure, the feasibility of implementing such strategies may be higher, though challenges such as public acceptance and environmental concerns must still be considered. In contrast, in developing countries, especially those in Sub-Saharan Africa where malaria remains a significant burden, the success of *Microsporidia MB*-based strategies may depend heavily on factors such as resource availability, healthcare access, and cultural acceptance of such interventions. Moreover, the effectiveness of these strategies could be influenced by local mosquito species, environmental conditions, and the presence of competing interventions. Therefore, while our model offers promising insights, its implementation will require careful consideration of local contexts. Several promising directions for future research in this field include the influence of seasonality on the life cycle of mosquitoes and the dynamics of symbiont spread. Investigating how seasonal variations affect transmission could provide valuable insights into timing interventions effectively. Additionally, exploring the spatial heterogeneity in the distribution of uninfected and infected mosquitoes could help optimize release strategies based on local environmental factors and mosquito population structures.

In conclusion, our mathematical model offers a powerful tool for studying the complex dynamics of *Microsporidia MB* infection in mosquitoes. Through our analysis, we have highlighted the significance of maternal transmission and release strategies in achieving population replacement. These insights have practical implications for the development of more effective interventions and control strategies against mosquito-borne diseases, ultimately reducing their impact on human health.

Appendix A Existence of the Coexistence Equilibrium

A.1 Coexistence Equilibrium

The search for this equilibrium point leads us to the solution of the following system:

$$\begin{cases} \phi\left(\dfrac{M_uF_u+(1-\rho_1)M_iF_i+(1-\rho_2)M_uF_i+(1-\rho_3\lambda_m)M_iF_u}{M_u+M_i}\right)\left(1-\dfrac{A}{K_a}\right) \\ -(\gamma+\mu_a)A_u=0, \\ \phi\left(\dfrac{\rho_1M_iF_i+\rho_2M_uF_i+\rho_3\lambda_mM_iF_u}{M_u+M_i}\right)\left(1-\dfrac{A}{K_a}\right)-(\gamma+\mu_a)A_i=0, \\ b_f\gamma A_u-\beta_m\frac{M_i}{M_u+M_i}F_u-\mu_fF_u=0, \\ b_f\gamma A_i+\beta_m\frac{M_i}{M_u+M_i}F_u-\mu_fF_i=0, \\ b_m\gamma A_u-\beta_f\frac{F_i}{F_u+F_i}M_u-\mu_mM_u=0, \\ b_m\gamma A_i+\beta_f\frac{F_i}{F_u+F_i}M_u-\mu_mM_i=0. \end{cases} \tag{A1}$$

Let us recall the following notations:

$$A=A_u+A_i,\quad F=F_u+F_i\quad et\quad M=M_u+M_i.$$

Then we obtain the system:

$$\begin{cases} \phi F\left(1-\dfrac{A}{K_a}\right)-(\gamma+\mu_a)A=0, \\ b_f\gamma A-\mu_fF=0, \\ b_m\gamma A-\mu_mM=0. \end{cases} \tag{A2}$$

The system (A2) admits for solution:

$$A=K_a\left(1-\frac{1}{\mathcal{R}_u}\right),\quad F=b_f\frac{\gamma}{\mu_f}A,\quad M=b_m\frac{\gamma}{\mu_m}A, \tag{A3}$$

satisfying the relation

$$M=lF,\quad \text{with}\quad l=\frac{b_m\mu_f}{b_f\mu_m}. \tag{A4}$$

By posing

$$p=\frac{M_i}{M_u+M_i}, \tag{A5}$$

we obtain from (A1), (A3), (A4) and (A4) the system:

$$\begin{cases} \dfrac{\phi}{\mathcal{R}_u}[(1-p)F_u+(1-\rho_1)pF_i+(1-\rho_2)(1-p)F_i+(1-\rho_3\lambda_m)pF_u] \\ -(\gamma+\mu_a)A_u=0, \\ \dfrac{\phi}{\mathcal{R}_u}[\rho_1pF_i+\rho_2(1-p)F_i+\rho_3\lambda_mpF_u]-(\gamma+\mu_a)A_i=0, \\ b_f\gamma A_u-\beta_mpF_u-\mu_fF_u=0, \\ b_f\gamma A_i+\beta_mpF_u-\mu_fF_i=0, \\ b_m\gamma A_u-\beta_fl(1-p)F_i-\mu_m(1-p)lF=0, \\ b_m\gamma A_i+\beta_fl(1-p)F_i-\mu_mlpF=0. \end{cases} \tag{A6}$$

Where $F = F_u + F_i$ and as a result, the last four allow us to have:

$$\begin{aligned} A_u &= \frac{\beta_m p + \mu_f}{b_f \gamma} F_u, \\ A_i &= \frac{p}{1-p}\left(\frac{\mu_f \alpha - (1-p)\beta_m}{b_f \gamma}\right) F_u, \\ F_i &= \alpha \frac{p}{1-p} F_u, \\ F_u &= K_a \frac{b_f \gamma}{\mu_f}\left(1 - \frac{1}{\mathcal{R}_u}\right)\left(\frac{1-p}{1-p+\alpha p}\right). \end{aligned} \tag{A7}$$

with

$$\alpha = \frac{\mu_m}{\mu_f}\left(\frac{\beta_m + \mu_f}{\beta_f + \mu_m}\right). \tag{A8}$$

Considering the expressions in (A7),the second equation in (A6), allows us to have

$$p = \frac{\beta_m - \alpha \mu_f (1 - \rho_2 - \rho_3 \lambda_m)}{\beta_m - \alpha \mu_f (\rho_1 - \rho_2 - \rho_3 \lambda_m)}. \tag{A9}$$

- When $\rho_1 = 1$, then $p = 1$. Replacing p with its value in the system (A6), we have $A_u = F_u = M_u = 0$ and thus we find the complete infection equilibrium point (CIE) given by (16).
- When $\rho_1 < 1$, we use the relations (A4) and (A5) to express M_u and M_i in terms of F_u and the unique solution of (A1) representing E^c is given by:

$$\begin{aligned} F_u^c &= K_a \frac{b_f \gamma}{\mu_f}\left(1 - \frac{1}{\mathcal{R}_u}\right)\left(\frac{1-p}{1-p+\alpha p}\right), \\ A_u^c &= \frac{\beta_m p + \mu_f}{b_f \gamma} F_u^c, \\ A_i^c &= \frac{p}{1-p}\left(\frac{\mu_f \alpha - (1-p)\beta_m}{b_f \gamma}\right) F_u^c, \\ F_i^c &= \alpha \frac{p}{1-p} F_u^c, \\ M_u^c &= (1 - p + \alpha p) l F_u^c, \\ M_i^c &= \frac{p}{1-p}(1 - p + \alpha p) l F_u^c. \end{aligned} \tag{A10}$$

The quantity p given by relation (A9), $(0 < p < 1)$ represents the proportion of infected males in the total population of males at equilibrium, i.e., $p = \dfrac{M_i^c}{M_u^c + M_i^c}$.

A.2 Existence of E^c

Proof It follows from expression (A10) that E^c is well defined in $\mathcal{D}$ if and only if:

$$F_u^c > 0, \quad \mu_f \alpha > (1-p)\beta_m \quad and \quad 0 < p < 1.$$

The condition $F_u^c > 0$ leads $\mathcal{R}_u > 1$.

$$\begin{aligned}
\mu_f\alpha > (1-p)\beta_m &\Leftrightarrow \rho_1\frac{\beta_m\beta_f}{\mu_m\mu_f} + (\rho_2+\rho_3\lambda_m)\frac{\beta_m}{\mu_f} + \rho_2 + \rho_3\lambda_m - \rho_1 > 0\\
&\Leftrightarrow \mathcal{T}_0 - 1 > -\left[\rho_3\lambda_m\left(\frac{\beta_m}{\mu_f} - \frac{\beta_f}{\mu_m}\right) + (1-\rho_1)\left(1 - \frac{\beta_m\beta_f}{\mu_m\mu_f}\right)\right]\\
&\Leftrightarrow (\mathcal{R}_0 - 1)d > -\left[\rho_3\lambda_m\left(\frac{\beta_m}{\mu_f} - \frac{\beta_f}{\mu_m}\right) + (1-\rho_1)\left(1 - \frac{\beta_m\beta_f}{\mu_m\mu_f}\right)\right]\\
&\Leftrightarrow \mathcal{R}_0 > 1 - \frac{1}{d}\left[\rho_3\lambda_m\left(\frac{\beta_m}{\mu_f} - \frac{\beta_f}{\mu_m}\right) + (1-\rho_1)\left(1 - \frac{\beta_m\beta_f}{\mu_m\mu_f}\right)\right] = \mathcal{R}_1.\\
0 < p < 1 &\Leftrightarrow \beta_m > \alpha\mu_f(1-\rho_2-\rho_3\lambda_m)\\
&\Leftrightarrow \frac{\beta_m\beta_f}{\mu_m\mu_f} + (\rho_2+\rho_3\lambda_m)\frac{\beta_m}{\mu_f} + \rho_2 + \rho_3\lambda_m - 1 > 0\\
&\Leftrightarrow \mathcal{T}_0 - 1 > -\rho_3\lambda_m\left(\frac{\beta_m}{\mu_f} - \frac{\beta_f}{\mu_m}\right)\\
&\Leftrightarrow (\mathcal{R}_0 - 1)d > -\rho_3\lambda_m\left(\frac{\beta_m}{\mu_f} - \frac{\beta_f}{\mu_m}\right)\\
&\Leftrightarrow \mathcal{R}_0 > 1 - \frac{\rho_3\lambda_m}{d}\left(\frac{\beta_m}{\mu_f} - \frac{\beta_f}{\mu_m}\right) = \mathcal{R}_0^*.
\end{aligned}$$

Therefore, we need $\mathcal{R}_0 > \max\{\mathcal{R}_0^*, \mathcal{R}_1\}$. According to the assumption (12), we have $\left(\frac{\beta_m}{\mu_f} - \frac{\beta_f}{\mu_m}\right) \geq 0$. Moreover, since $\frac{\beta_m}{\mu_m}.\frac{\beta_f}{\mu_f} < 1$ and so the condition of existence of the equilibrium E_c comes down to $\mathcal{R}_u > 1$ and $\mathcal{R}_0 > \mathcal{R}_0^*$.

Furthermore, the expressions in the numerator and denominator of p in the expression (A9) are rewritten as follows:

$$\begin{aligned}
\beta_m - \alpha\mu_f(1-\rho_2-\rho_3\lambda_m) &= \frac{\mu_m\mu_f}{\beta_f+\mu_m}\left(\frac{\beta_m\beta_f}{\mu_m\mu_f} + (\rho_2+\rho_3\lambda_m)\frac{\beta_m}{\mu_f} + \rho_2 + \rho_3\lambda_m - 1\right)\\
&= \frac{\mu_m\mu_f}{\beta_f+\mu_m}(\mathcal{R}_0 - \mathcal{R}_0^*)d, \quad \text{and}\\
\beta_m - \alpha\mu_f(\rho_1-\rho_2-\rho_3\lambda_m) &= \frac{\mu_m\mu_f}{\beta_f+\mu_m}\left(\frac{\beta_m\beta_f}{\mu_m\mu_f} + (1-\rho_1+\rho_2+\rho_3\lambda_m)\frac{\beta_m}{\mu_f}\right)\\
&\quad + \frac{\mu_m\mu_f}{\beta_f+\mu_m}(\rho_2+\rho_3\lambda_m-\rho_1)\\
&= \frac{\mu_m\mu_f}{\beta_f+\mu_m}\left(\mathcal{R}_0 - \mathcal{R}_0^* + \frac{1-\rho_1}{d}\left(1+\frac{\beta_m}{\mu_f}\right)\right)d.
\end{aligned}$$

Thus the expression for p given by relation (A9) becomes:

$$p = \frac{\beta_m - \alpha\mu_f(1-\rho_2-\rho_3\lambda_m)}{\beta_m - \alpha\mu_f(\rho_1-\rho_2-\rho_3\lambda_m)} = \frac{\mathcal{R}_0 - \mathcal{R}_0^*}{\mathcal{R}_0 - \mathcal{R}_0^* + \frac{1-\rho_1}{d}\left(1+\frac{\beta_m}{\mu_f}\right)}.$$

□

Appendix B Local Stability of E_u and E_i When $\rho_1 = 1$

The proof of the local stability of the equilibrium points E_u and E_i are similar and we only provide here that of E_u.

Proof To prove stability, we use the known results on Metzler matrices [34]. The Jacobian matrix of (2) at the point E_u is given by:

$$J(E_u) = \begin{pmatrix} -(\gamma+\mu_a)\mathcal{R}_u & (\gamma+\mu_a)(1-\mathcal{R}_u) & \frac{\phi}{\mathcal{R}_u} & (1-\rho_2)\frac{\phi}{\mathcal{R}_u} & 0 & -\rho_3\lambda_m\frac{\phi}{\mathcal{R}_u}\frac{F_u^*}{M_u^*} \\ 0 & -(\gamma+\mu_a) & 0 & \rho_2\frac{\phi}{\mathcal{R}_u} & 0 & \rho_3\lambda_m\frac{\phi}{\mathcal{R}_u}\frac{F_u^*}{M_u^*} \\ b_f\gamma & 0 & -\mu_f & 0 & 0 & -\beta_m\frac{F_u^*}{M_u^*} \\ 0 & b_f\gamma & 0 & -\mu_f & 0 & \beta_m\frac{F_u^*}{M_u^*} \\ b_m\gamma & 0 & 0 & -\beta_f\frac{M_u^*}{F_u^*} & -\mu_m & 0 \\ 0 & b_m\gamma & 0 & \beta_f\frac{M_u^*}{F_u^*} & 0 & -\mu_m \end{pmatrix}.$$

This gives us

$$\begin{aligned} &\det(J(E_u) - xI_6) \\ &= \begin{vmatrix} -(\gamma+\mu_a)\mathcal{R}_u - x & (\gamma+\mu_a)(1-\mathcal{R}_u) & \frac{\phi}{\mathcal{R}_u} & (1-\rho_2)\frac{\phi}{\mathcal{R}_u} & 0 & -\rho_3\lambda_m\frac{\phi}{\mathcal{R}_u}\frac{F_u^*}{M_u^*} \\ 0 & -(\gamma+\mu_a) - x & 0 & \rho_2\frac{\phi}{\mathcal{R}_u} & 0 & \rho_3\lambda_m\frac{\phi}{\mathcal{R}_u}\frac{F_u^*}{M_u^*} \\ b_f\gamma & 0 & -\mu_f - x & 0 & 0 & -\beta_m\frac{F_u^*}{M_u^*} \\ 0 & b_f\gamma & 0 & -\mu_f - x & 0 & \beta_m\frac{F_u^*}{M_u^*} \\ b_m\gamma & 0 & 0 & -\beta_f\frac{M_u^*}{F_u^*} & -\mu_m - x & 0 \\ 0 & b_m\gamma & 0 & \beta_f\frac{M_u^*}{F_u^*} & 0 & -\mu_m - x \end{vmatrix} \\ &= -(x+\mu_m)\left|\begin{array}{cc|ccc} -(\gamma+\mu_a)\mathcal{R}_u - x & \frac{\phi}{\mathcal{R}_u} & (\gamma+\mu_a)(1-\mathcal{R}_u) & (1-\rho_2)\frac{\phi}{\mathcal{R}_u} & -\rho_3\lambda_m\frac{\phi}{\mathcal{R}_u}\frac{F_u^*}{M_u^*} \\ b_f\gamma & -\mu_f - x & 0 & 0 & -\beta_m\frac{F_u^*}{M_u^*} \\ \hline 0 & 0 & -(\gamma+\mu_a) - x & \rho_2\frac{\phi}{\mathcal{R}_u} & \rho_3\lambda_m\frac{\phi}{\mathcal{R}_u}\frac{F_u^*}{M_u^*} \\ 0 & 0 & b_f\gamma & -\mu_f - x & \beta_m\frac{F_u^*}{M_u^*} \\ 0 & 0 & b_m\gamma & \beta_f\frac{M_u^*}{F_u^*} & -\mu_m - x \end{array}\right|. \end{aligned}$$

Thus, the characteristic polynomial associated with $J(E_u)$ is given by:

$$P_1(x) = -(x+\mu_m)\det(M_1 - xI_2)\det(N_1 - xI_3).$$

Where

$$M_1 = \begin{pmatrix} -(\gamma+\mu_a)\mathcal{R}_u & \frac{\phi}{\mathcal{R}_u} \\ b_f\gamma & -\mu_f \end{pmatrix}, \text{ and}$$

$$N_1 = \left(\begin{array}{cc|c} -(\gamma+\mu_a) & \rho_2\frac{\phi}{\mathcal{R}_u} & \rho_3\lambda_m\frac{\phi}{\mathcal{R}_u}\frac{F_u^*}{M_u^*} \\ b_f\gamma & -\mu_f & \beta_m\frac{F_u^*}{M_u^*} \\ \hline b_m\gamma & \beta_f\frac{M_u^*}{F_u^*} & -\mu_m \end{array}\right) = \left(\begin{array}{c|c} A_1 & B_1 \\ \hline C_1 & D_1 \end{array}\right).$$

Then $Sp(J(E_u)) = \{-\mu_m\} \cup Sp(M_1) \cup Sp(N_1)$. It is therefore sufficient to study the stability of matrices N_1 and M_1.

M_1 eis a Metzler matrix. Since all diagonal terms are fully negative, it is Metzler stable if and only if $\det M_1 = (\gamma + \mu_a)\mu_f(\mathcal{R}_u - 1) > 0$ i.e if $\mathcal{R}_u > 1$.

N_1 is a Metzler matrix and it is Metzler stable if and only if A_1 and $D_1 - C_1 A_1^{-1} B_1$ are Metzler stable [34]. A_1 is a stable Metzler matrix because all its non diagonal terms are positive, its diagonal terms all negative and $\det A_1 = (\gamma + \mu_a)\mu_f(1 - \rho_2) > 0$. Moreover,

$$\begin{aligned} D_1 - C_1 A_1^{-1} B_1 &= -\frac{\mu_m}{1-\rho_2}\left(1 - \rho_2 - \rho_3\lambda_m - \rho_2\frac{\beta_m}{\mu_f} - \rho_3\lambda_m\frac{\beta_f}{\mu_m} - \frac{\beta_m\beta_f}{\mu_m\mu_f}\right) \\ &= -\frac{\mu_m}{1-\rho_2}(1 - \mathcal{T}_0) < 0 \quad \text{if} \quad \mathcal{T}_0 < 1. \end{aligned}$$

This condition is equivalent to $\mathcal{R}_0 < 1$ from i) of Proposition 2 and thus N_1 is a stable Metzler matrix. □

Author Contributions DT: conceptualization, methodology, formal analysis, software, writing—original draft preparation, writing—reviewing and editing. BT: conceptualization, methodology, formal analysis, supervison, writing—reviewing and editing. JL: writing—reviewing and editing. MD: writing—reviewing and editing.

Funding BT Acknowledges with thanks the support of the NRF Incentive Funding for Rated Researcher (NRF-IPRR), Grant number RA201218580317, and the support of the French Institute of Research for Development (IRD) through UMMISCO and its 2022 MLD Programme.

Availability of data and materials Not applicable.

Declarations

Conflict of interest The authors declare no conflict of interest

References

1. Camejo, A.: Control issues. Trends Parasitol. **32**(3), 169–171 (2016)
2. Organization, W.H., et al.: A global brief on vector-borne diseases. World Health Organization, Technical report (2014)
3. Santé, O., Organization, W.H.: Progress towards regional measles elimination–worldwide, 2000–2019–progrès accomplis dans le monde en vue de l'élimination régionale de la rougeole, 2000-2019. Weekly Epidemiological Record= Relevé épidémiologique hebdomadaire 95(46), 564–572 (2020)
4. Adekunle, A.I., Meehan, M.T., McBryde, E.S.: Mathematical analysis of a wolbachia invasive model with imperfect maternal transmission and loss of wolbachia infection. Infectious Disease Modelling **4**, 265–285 (2019)
5. Qu, Z., Xue, L., Hyman, J.M.: Modeling the transmission of wolbachia in mosquitoes for controlling mosquito-borne diseases. SIAM J. Appl. Math. **78**(2), 826–852 (2018)
6. Bian, G., Xu, Y., Lu, P., Xie, Y., Xi, Z.: The endosymbiotic bacterium wolbachia induces resistance to dengue virus in aedes aegypti. PLoS Pathog. **6**(4), 1000833 (2010)
7. Moreira, L.A., Iturbe-Ormaetxe, I., Jeffery, J.A., Lu, G., Pyke, A.T., Hedges, L.M., Rocha, B.C., Hall-Mendelin, S., Day, A., Riegler, M.: A wolbachia symbiont in aedes aegypti limits infection with dengue, chikungunya, and plasmodium. Cell **139**(7), 1268–1278 (2009)
8. Hu, L., Yang, C., Hui, Y., Yu, J.: Mosquito control based on pesticides and endosymbiotic bacterium wolbachia. Bull. Math. Biol. **83**(5), 1–24 (2021)
9. Zhang, X., Liu, Q., Zhu, H.: Modeling and dynamics of wolbachia-infected male releases and mating competition on mosquito control. J. Math. Biol. **81**(1), 243–276 (2020)
10. Zheng, B., Tang, M., Yu, J.: Modeling wolbachia spread in mosquitoes through delay differential equations. SIAM J. Appl. Math. **74**(3), 743–770 (2014)
11. Almeida, L., Duprez, M., Privat, Y., Vauchelet, N.: Mosquito population control strategies for fighting against arboviruses. Math. Biosci. Eng. **16**(6), 6274–6297 (2019)

12. Campo-Duarte, D.E., Vasilieva, O., Cardona-Salgado, D., Svinin, M.: Optimal control approach for establishing wmelpop wolbachia infection among wild aedes aegypti populations. J. Math. Biol. **76**(7), 1907–1950 (2018)
13. Zheng, B., Guo, W., Hu, L., Huang, M., Yu, J.: Complex wolbachia infection dynamics in mosquitoes with imperfect maternal transmission. Mathematical Biosciences & Engineering **15**(2), 523 (2018)
14. Zheng, B., Tang, M., Yu, J., Qiu, J.: Wolbachia spreading dynamics in mosquitoes with imperfect maternal transmission. J. Math. Biol. **76**(1), 235–263 (2018)
15. Andreychuk, S., Yakob, L.: Mathematical modelling to assess the feasibility of wolbachia in malaria vector biocontrol. J. Theor. Biol. **542**, 111110 (2022)
16. Florez, D., Young, A.J., Bernabé, K.J., Hyman, J.M., Qu, Z.: Modeling sustained transmission of wolbachia among anopheles mosquitoes: implications for malaria control in haiti. Tropical Medicine and Infectious Disease **8**(3), 162 (2023)
17. Herren, et al.: A microsporidian impairs plasmodium falciparum transmission in anopheles arabiensis mosquitoes. Nature communications 11(1), 1–10 (2020)
18. Nattoh, G., Maina, T., Makhulu, E.E., Mbaisi, L., Mararo, E., Otieno, F.G., Bukhari, T., Onchuru, T.O., Teal, E., Paredes, J., et al.: Horizontal transmission of the symbiont microsporidia mb in anopheles arabiensis. Frontiers in Microbiology **12** (2021)
19. Ogunlade, et al.: Modeling the potential of w au-wolbachia strain invasion in mosquitoes to control aedes-borne arboviral infections. Scientific Reports 10(1), 1–16 (2020)
20. Anguelov, R., Dumont, Y., Lubuma, J.: Mathematical modeling of sterile insect technology for control of anopheles mosquito. Computers & Mathematics with Applications **64**(3), 374–389 (2012)
21. Carrington, L.B., Lipkowitz, J.R., Hoffmann, A.A., Turelli, M.: A re-examination of wolbachia-induced cytoplasmic incompatibility in california drosophila simulans. PLoS ONE **6**(7), 22565 (2011)
22. Chitnis, N., Hyman, J.M., Cushing, J.M.: Determining important parameters in the spread of malaria through the sensitivity analysis of a mathematical model. Bull. Math. Biol. **70**(5), 1272–1296 (2008)
23. Qu, Z., Hyman, J.M.: Generating a hierarchy of reduced models for a system of differential equations modeling the spread of wolbachia in mosquitoes. SIAM J. Appl. Math. **79**(5), 1675–1699 (2019)
24. Almeida, L., Privat, Y., Strugarek, M., Vauchelet, N.: Optimal releases for population replacement strategies: application to wolbachia. SIAM J. Math. Anal. **51**(4), 3170–3194 (2019)
25. Driessche, P., Watmough, J.: Reproduction numbers and sub-threshold endemic equilibria for compartmental models of disease transmission. Math. Biosci. **180**(1–2), 29–48 (2002)
26. Hethcote, H.W.: The mathematics of infectious diseases. SIAM Rev. **42**(4), 599–653 (2000)
27. Lewis, M.A., Shuai, Z., Driessche, P.: A general theory for target reproduction numbers with applications to ecology and epidemiology. J. Math. Biol. **78**, 2317–2339 (2019)
28. Liana, Y.A., Shaban, N., Mlay, G.: Modeling optimal control of african trypanosomiasis disease with cost-effective strategies. J. Biol. Syst. **29**(04), 823–848 (2021)
29. Fleming, W.H., Rishel, R.W.: Deterministic and Stochastic Optimal Control vol. 1. Springer (2012)
30. Lukes, D.L.: Differential Equations: Classical to Controlled vol. 162. Academic press New York (1982)
31. Lenhart, S., Workman, J.T.: Optimal Control Applied to Biological Models. Chapman and Hall/CRC (2007)
32. Pontryagin, L., Boltyanskii, V.: Rv gamkrelidze and ef mishenko, the mathematical theory of optimal processes. New York (1962)
33. Beal, L., Hill, D., Martin, R., Hedengren, J.: Gekko optimization suite. Processes **6**(8), 106 (2018). https://doi.org/10.3390/pr6080106
34. Kamgang, J.C., Sallet, G.: Computation of threshold conditions for epidemiological models and global stability of the disease-free equilibrium (dfe). Math. Biosci. **213**(1), 1–12 (2008)